

Gold *Manno*-Glyconanoparticles: Multivalent Systems to Block HIV-1 gp120 Binding to the Lectin DC-SIGN⁺

Olga Martínez-Ávila,^[a] Karolin Hijazi,^[b] Marco Marradi,^[a] Caroline Clavel,^[a, c] Colin Campion,^[d] Charles Kelly,^[b] and Soledad Penadés*^[a]

Abstract: The HIV envelope glycoprotein gp120 takes advantage of the high-mannose clusters on its surface to target the C-type lectin dendritic cell-specific intracellular adhesion molecule-3-grabbing non-integrin (DC-SIGN) on dendritic cells. Mimicking the cluster presentation of oligomannosides on the virus surface is a strategy for designing carbohydrate-based antiviral agents. Bio-inspired by the cluster presentation of gp120, we have designed and prepared a small library of multivalent water-soluble gold glyconanoparticles (*manno*-GNPs) presenting truncated (oligo)mannosides of the high-mannose undecasaccharide Man₆GlcNAc₂ and have tested them as inhibitors of DC-SIGN binding to

gp120. These glyconanoparticles are ligands for DC-SIGN, which also interacts in the early steps of infection with a large number of pathogens through specific recognition of associated glycans. (Oligo)mannosides endowed with different spacers ending in thiol groups, which enable attachment of the glycoconjugates to the gold surface, have been prepared. *manno*-GNPs with different spacers and variable density of mannose (oligo)saccharides have been obtained and characterized. Surface

Keywords: glycoconjugates • glyconanoparticles • high-mannose oligosaccharides • multivalency • surface-plasmon resonance

plasmon resonance (SPR) experiments with selected *manno*-GNPs have been performed to study their inhibition potency towards DC-SIGN binding to gp120. The tested *manno*-GNPs completely inhibit the binding from the micro- to the nanomolar range, while the corresponding monovalent mannosides require millimolar concentrations. *manno*-GNPs containing the disaccharide Man α 1-2Man α are the best inhibitors, showing more than 20000-fold increased activity (100% inhibition at 115 nM) compared to the corresponding monomeric disaccharide (100% inhibition at 2.2 mM). Furthermore, increasing the density of dimannoside on the gold platform from 50 to 100% does not improve the level of inhibition.

Introduction

Multivalency is ubiquitous in biological interactions, including carbohydrate-mediated processes.^[1] The low affinity of

carbohydrate-mediated interactions is compensated by clustering of the ligands. Multivalency is essential in carbohydrate–protein interactions.^[2] Different chemical approaches have been developed to study carbohydrate interactions, all

[a] Dr. O. Martínez-Ávila, Dr. M. Marradi, Dr. C. Clavel, Prof. Dr. S. Penadés
Laboratory of GlycoNanotechnology
Biofunctional Nanomaterial Unit
CIC biomaGUNE and CIBER-BBN
Parque Tecnológico, Pº de Miramón 182, 20009 San Sebastián (Spain)
Fax: (+34) 943 00 53 01
E-mail: spenades@cicbiomagune.es

[b] Dr. K. Hijazi, Prof. C. Kelly
King's College London, Dental Institute, Oral Immunology
Tower Wing, Guy's Hospital, London, SE1 9RT (UK)

[c] Dr. C. Clavel
Current address: IBMM, UMR 5247
CNRS-Universités Montpellier 2 et 1
ENSCM, rue de l'École Normale 8
34296 Montpellier Cedex 5 (France)

[d] Dr. C. Campion
Carbohydrate Synthesis Ltd., Abingdon (UK)

[*] DC-SIGN = Dendritic cell-specific intracellular adhesion molecule-3-grabbing non-integrin.

Supporting information for this article is available on the WWW under <http://dx.doi.org/10.1002/chem.200900923>. Synthesis and characterization of neoglycoconjugates GlcC₅S and **14–16**, linkers **26, 39**, and **40**, aminoethyl mannosides **27–32**, and main intermediates; preparation and characterization of GlcC₅-Au and HO₂C-Au GNPs; TEM histograms and size distribution of GNPs **4–7, 8, 9 a,b, 10 a,b, 11 a,b, 12 a,b**, and **13 a**, glcC₅-Au, and HO₂C-Au; ¹H and ¹³C NMR spectra of neoglycoconjugates **16, 33–38**, GlcC₅S, and linkers **26, 39**, and **40**. Sensorgrams (Figures S1–S4) of SPR experiments.

of which are based on multivalent presentation of carbohydrate ligands.^[3]

We have developed new polyvalent systems (glyconanoparticles) consisting of a metallic core, to which self-assembled monolayers of glycoconjugates are covalently linked.^[4–6] Glyconanoparticles (GNPs) are water-soluble bio-functional gold nanoclusters with a three-dimensional (3D) polyvalent carbohydrate display and globular shape, chemically well-defined composition, and an exceptionally small core size. They can display a large number of carbohydrates on a reduced surface with a high local concentration of sugars (100 molecules on a 2 nm core gold) or lower densities. GNPs are useful tools for investigating carbohydrate-mediated interactions.^[7,8] GNPs functionalized with lactose neoglycoconjugates have been shown to be efficient anti-adhesion agents, inhibiting the *ex vivo* metastasis of melanoma in mice by up to 70%.^[8]

The surface unit of the HIV envelope glycoprotein gp120 is heavily glycosylated with *N*-linked mannose glycans,^[9] which presumably shield the neutralizing epitopes.^[10] Despite the large variation in the amino acid sequence of gp120 due to the immune selective pressure, the overall degree of glycosylation is preserved.^[11] The C-type lectin DC-SIGN (dendritic cell-specific intracellular adhesion molecule-3 (ICAM-3)-grabbing non-integrin) expressed on the surface of dermal dendritic cells (DCs) has been implicated in HIV vaginal transmission.^[12–14] DC-SIGN binds specifically to the oligomannosides on gp120 through protein–carbohydrate interactions in a multivalent and Ca²⁺-dependent manner.^[15–17] Carbohydrate structures on gp120 are targets for candidate antiviral agents and vaccines.^[18–21] Mimicking the cluster presentation of the oligomannosides on the virus surface is a strategy for designing carbohydrate-based antiviral agents. Multivalent systems of mannose oligosaccharides based on proteins,^[22] peptides,^[23,24] dendrimers,^[25,26] and other scaffolds have been prepared and tested as inhibitors of gp120 binding to DC-SIGN or to monoclonal antibody 2G12. GNPs that interfere with gp120 interaction to DC-SIGN may prevent infection by inhibiting DC-mediated transmission of HIV to CD4 T cells.

The glyconanoparticle platform offers advantageous alternatives to protein, polymer, or dendrimer scaffolds. Glyconanoparticle technology (glyconanotechnology) allows the preparation of a great variety of water-soluble glycoclusters with different ligand densities (high and low loadings) and variable linkers to modulate rigidity and flexibility and to confer accessibility to the ligands.^[5] The nature (hydrophilic or hydrophobic), the length, and the flexibility of the spacer can be selected to control the presentation of the carbohydrates on the cluster surface, which influences their accessibility to the ligands and behaviour during molecular recognition events. Furthermore, glyconanotechnology offers the unique possibility of simultaneous incorporation, in a single gold cluster, of different ligands in a controlled way.^[27]

In this study, GNPs coated with sets of different structural motifs of the *N*-linked high-mannose-type glycans of gp120 have been designed to assess the effect of presentation on

the gold cluster and dissect the structural requirements of the sugars involved in HIV/DC-SIGN interaction. We present the preparation and characterization of a small library of water-soluble gold glyconanoparticles (*manno*-GNPs) functionalized with partial structures of the high-mannose undecasaccharide Man₉(GlcNAc)₂ of gp120 or with a non-natural heptasaccharide (Figure 1). The (oligo)mannosides were endowed with different spacers ending in a mercapto (thiol) group, which enables attachment of the glycoconjugates to the gold surface. *Manno*-GNPs with different spacers and variable density of mannose (oligo)saccharides have been prepared and explored (Figure 1). Selected glyconanoparticles bearing the (oligo)mannosides have been tested as inhibitors of DC-SIGN binding to gp120 by surface plasmon resonance (SPR). We show that multivalent presentation of a simple Man α 1-2Man α disaccharide on the gold nanoparticle increases the inhibitory activity by more than four orders of magnitude compared to the monovalent disaccharide. Furthermore, increasing the density of dimannoside on the gold platform does not improve the inhibitory potency.

Results and Discussion

Multivalent systems functionalized with oligomannosides have recently been designed as potential vaccines against HIV or to provide insights into understanding HIV glycobiochemistry.^[19–23,28] Multivalent Man₉ clusters^[29] and template-assembled oligomannose clusters^[23,30] have been prepared and some of these systems proved more effective in inhibiting 2G12 binding to gp120 than the corresponding subunits.^[22,29b,30] It was also demonstrated that glycoclusters containing dimannosides were taken up avidly by dendritic cells.^[24,32]

Preparation of *manno*-GNPs **1–13** (Figure 1) requires conjugation of the (oligo)mannosides to a spacer ending in a mercapto (thiol) group. The selected (oligo)saccharides and the corresponding conjugates are displayed in Figure 2. They are structural motifs of the undecasaccharide Man₉(GlcNAc)₂, except for the heptasaccharide **32**, which results from adding two mannose residues to the pentasaccharide **31**. A major effort has been undertaken to develop efficient strategies for synthesizing high-mannose oligosaccharidic structures on gp120.^[32] Different protocols have been chosen for the preparation of the (oligo)mannose conjugates. To prepare the glycoconjugates, diverse spacers in terms of their hydrophobic and/or hydrophilic nature have been used: aliphatic chains (C₂ or C₅) to impart rigidity to the GNP, or an amphiphilic mixed aliphatic/polyethylene glycol linker to impart flexibility and solubility to the nanoparticle. The spacers have been introduced in the sugar either by direct glycosylation or by conjugation of alkylamino-functionalized (oligo)saccharides to a linker endowed with either a carboxylic or an isothiocyanate group. The preparation of neoglycoconjugates of biologically relevant sugars requires the development of efficient conjugation protocols

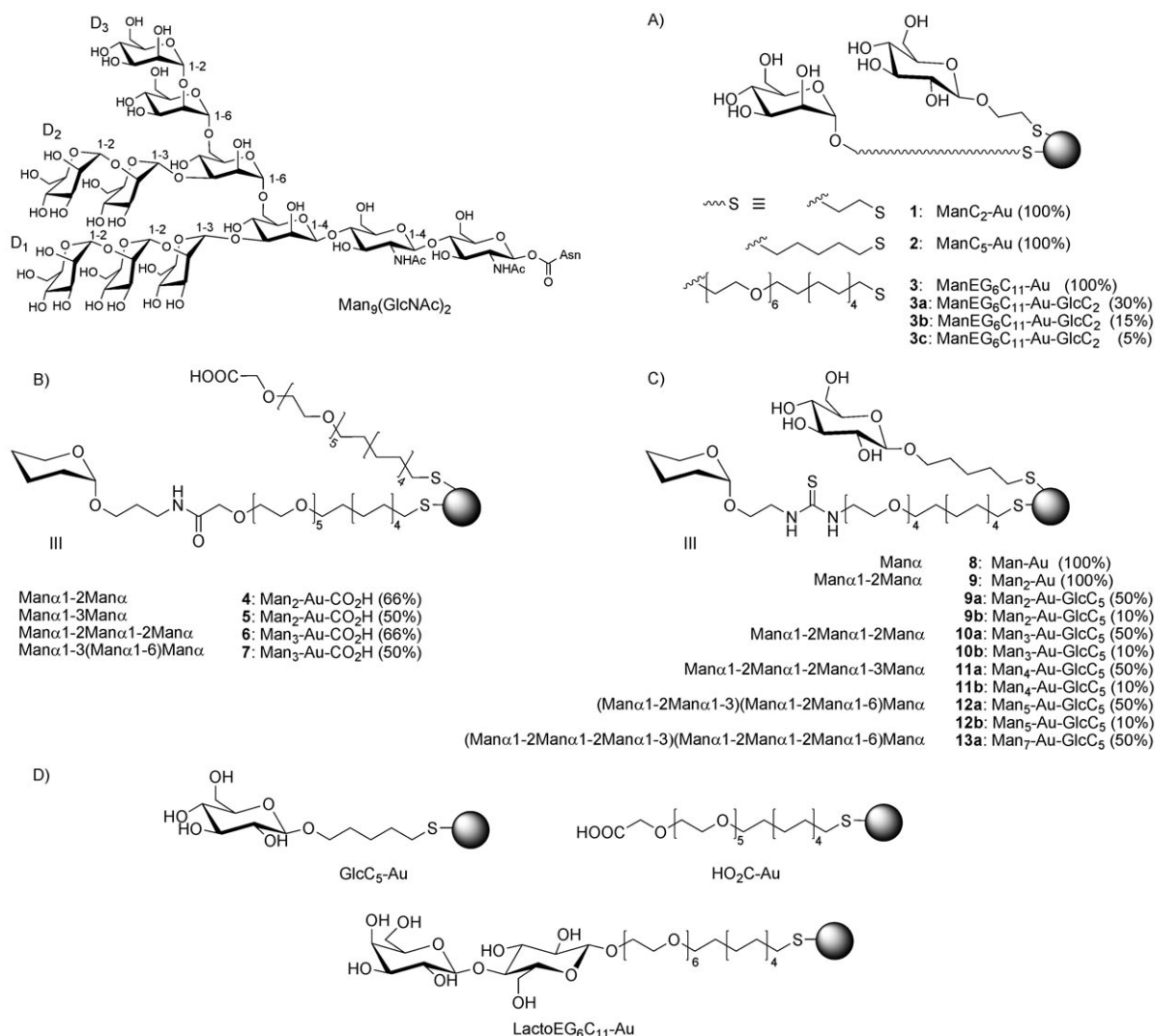


Figure 1. Structure of the high-mannose glycans and schematic representation of gold *manno*-glyconanoparticles (A, B, and C) and the control nanoparticles (D).

for attaching the carbohydrates to the different linkers. Easy and standard procedures can be applied for mono- and disaccharides, but as the complexity of the sugar increases, the necessity of setting up a general methodology to obtain various neoglycoconjugates with suitable thiol-terminated linkers on a laboratory scale becomes a real challenge. Different conjugation methods have been used to obtain the sugar conjugates. The monosaccharide conjugates **14–16** (Figure 2A) were prepared by direct glycosylation of the conveniently protected sugar with the appropriate linkers. Because of the difficulty of applying this strategy to oligosaccharides, we tried a more versatile approach.

We prepared a series of alkylamino (oligo)mannosides (**18–21** and **27–32**) for further coupling with suitably functionalized amphiphilic linkers **26** and **39** (Figure 2B and C). Peptidic coupling between the amino derivatives and carboxylic acid-bearing linker **26** was only partially satisfactory, due to the formation of mixed disulfides and the requirement for an excess of the (oligo)saccharide. Coupling of the

amino-functionalized sugars with isothiocyanate-terminated linker **39** provided a solution. The latter coupling method allowed great versatility in linker selection as well as the preparation of an entire set of mono-, di-, tri-, tetra-, penta-, and heptamannoside GNPs (Figure 2C) in high yields.

The resulting glycoconjugates were incorporated at varying densities onto the surface of the gold nanoclusters. Three families of *manno*-GNPs, **1–3**, **4–7**, and **8–13**, were generated with mannose glycoconjugates obtained by direct glycosylation (Figure 1A), peptidic coupling (Figure 1B), and isothiocyanate coupling (Figure 1C), respectively. The density of (oligo)saccharides was controlled by adjusting the initial concentration of glycoconjugate with mixed linker **40** (HO₂CCH₂OEG₃C₁₁SH) or glucose conjugates 2,2'-dithio-bis(ethyl)- or 5,5'-dithio-bis(pentyl)- β -D-glucopyranoside (GlcC₂S or GlcC₅S) as stealth components. Glucose was chosen as a biocompatible inert component. Large terminal ligands, such as oligosaccharides, attached to a short alkane-thiol may induce disorder in the system.^[33] For (oligo)man-

water, ensures accessibility to ligands and assists water solubility. Furthermore, SAMs that present poly(ethylene glycol) units are known to resist the adsorption of proteins.^[34,35]

Preparation of neoglycoconjugates by direct glycosylation:

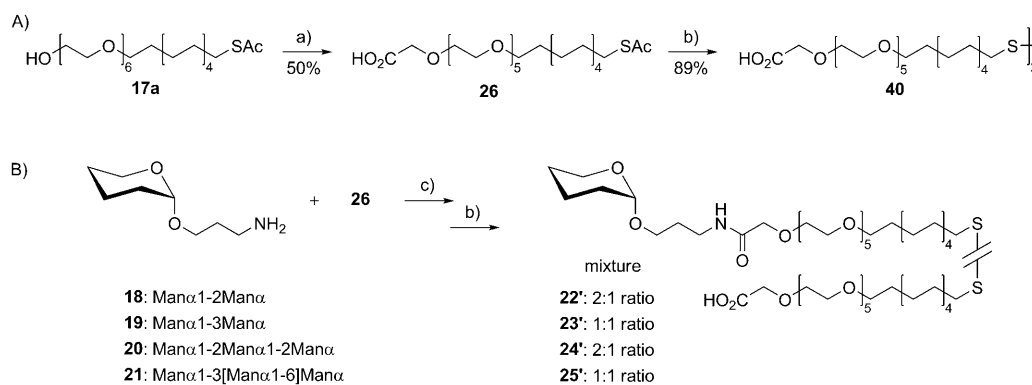
Mannose conjugates **14–16** (Figure 2A), 2,2'-dithio-bis(ethyl)- β -D-glucopyranoside (Glc₂S), 5,5'-dithio-bis(pentyl)- β -D-glucopyranoside (Glc₅S), and the lactose conjugate LactoEG₆C₁₁S were synthesized by direct glycosylation of the conveniently protected saccharides. The mannose conjugate **14**, functionalized with a two-carbon-atom chain, was prepared as previously reported with minor modifications.^[36] The mannose glycoconjugate **15**^[37] was prepared by a synthetic approach based on Fisher glycosylation.^[38] For the preparation of the neoglycoconjugate **16**, the peracetylated bromo-mannoside^[39] was glycosylated with the spacer **17a**^[40] in the presence of Hg(CN)₂ as a promoter^[41] to give the thioacetyl neoglycoconjugate, which was deacetylated by methanolysis^[42] to yield compound **16** (see the Supporting Information). The neoglycoconjugate GlcC₂S was synthesized as previously reported.^[27] Glucose functionalized with five carbon atoms GlcC₅S was efficiently produced by methanolysis of the corresponding thioacetate derivative, which was in turn prepared as reported in the literature.^[43] The conjugate LactoEG₆C₁₁S has been previously synthesized in our laboratory.^[5]

Due to the modest yields obtained with the direct glycosylation method, especially when mixed linkers were used, we investigated an alternative strategy for the synthesis of glycoconjugates **22–25** and **33–38**. We chose an approach in which fully deprotected 1-aminoalkyl glycosides were coupled to the linkers in the final steps. This is a convenient strategy, particularly when oligosaccharides are involved. The carboxylic acid- or isothiocyanate-functionalized linkers **26** and **39** were introduced by peptidic coupling or thiourea linkage formation. In principle, this also allows a greater versatility in terms of the spacer arms that can be incorporated.

Preparation of neoglycoconjugates by peptidic coupling:

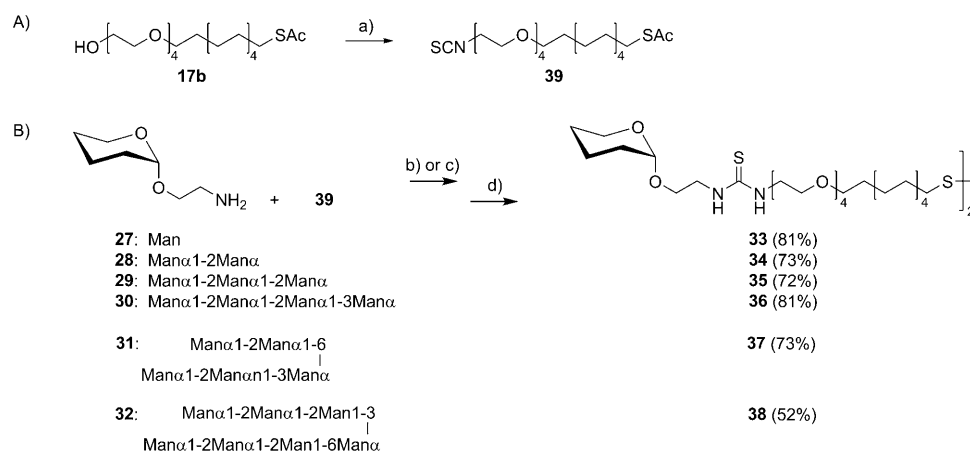
The neoglycoconjugates **22–25** (Figure 2B) were prepared from the aminopropyl mannosides **18–21** (provided as acetate salts) by peptidic coupling with carboxylated linker **26**, which was in turn synthesized by Jones oxidation^[44] of linker **17a**. Methanolysis of **26** afforded deprotected linker **40** (Scheme 1A). Conjugation of the unprotected aminopropyl glycosides **18–21** with the carboxylic linker **26** in DMF using diisopropylcarbodiimide (DIC) and 1-hydroxybenzotriazole (HOBt)^[45] resulted in a mixture of products (Scheme 1B).

Purification on Sephadex LH-20 was used to remove excess aminosugars, derivatives of the coupling reagents, and their sub-products. The integrals of the signal of the thioacetyl group (singlet at around $\delta=2.3$ ppm) in the ¹H NMR spectra were, in all cases, lower than expected, indicating that the reaction conditions caused partial deprotection of the thioacetyl group with consequent formation of mixed disulfide species. Furthermore, a sharp singlet at around $\delta=4.3$ ppm due to the methylene protons α to the carboxylic acid groups was detected, suggesting the presence of free carboxylic acid linker derivatives. Attempts to purify mixtures **22'–25'** by chromatography on silica gel were also unsuccessful: products **22–25** could not be isolated and a great loss of material occurred. Each mixture was thus directly treated with an excess of sodium methoxide to complete the deprotection of the thioacetyl group. After desalting on a column of Sephadex LH-20, a 2:1 mannose/carboxylic acid ratio for mixtures **22'** and **24'** or a 1:1 ratio for mixtures **23'** and **25'** (Scheme 1B) was determined by integration of the NMR signals of the anomeric protons of the mannoses and the methylene protons α to the carboxylic group. These mixtures were used to synthesize hybrid GNPs. The density of the ligands was conserved in the GNPs. Because of purification problems, the slow coupling reaction (24–48 h), and the requirement for an excess of amino saccharide, we investigated alternative synthetic methods. A parallel strategy based on the coupling of amino glycosides with an isothiocyanate-functionalized linker to form a thiourea linkage was used.



Scheme 1. Synthesis of A) linker **26** and B) neoglycoconjugates by peptidic coupling. a) CrO₃, H₂SO₄, acetone; b) MeONa, MeOH; c) HOBt, DIC, NEt₃, DMF.

Preparation of neoglycoconjugates by formation of a thiourea linkage: The neoglycoconjugates **33–38** (Figure 2C) were prepared by coupling of the aminoethyl (oligo)mannosides **27–32** with the isothiocyanate linker **39** (Scheme 2). The formation of a thiourea linkage between an amino group and an isothiocyanate group is a well-established reaction in bioconjugation that results in high yields of neoglycoconjugates.



Scheme 2. Synthesis of A) isothiocyanate linker **39** and B) (oligo)mannose neoglycoconjugates by thiourea formation. a) NaN_3 , PPh_3 , BrCCl_3 , DMF; then CS_2 , PPh_3 (72%, overall yield); b) NEt_3 , MeOH or c) NEt_3 , $i\text{PrOH}/\text{CH}_3\text{CN}/\text{H}_2\text{O}$ 1:1:1; d) MeONa , MeOH.

The aminoethyl monosaccharide **27** was synthesized in three steps from the commercial peracetylated mannose: standard glycosylation with 2-*N*-*Z*-ethanolamine in the presence of $\text{BF}_3 \cdot \text{Et}_2\text{O}$, deacetylation, followed by hydrogenation of the benzyloxycarbonyl group^[46] (see the Supporting Information). The aminoethyl mannosides **28** and **29** were obtained by glycosidation of thiotolyl di- and trimannoside donors, prepared by Wong's one-pot self-condensation strategy,^[32] with 2-*N*-*Z*-ethanolamine as the acceptor. The 1-aminoalkyl oligomannosides **30–32** were also synthesized by Wong's protocol, by glycosylation of thiotolyl di- and trimannoside donors with the ethylamino mannoside building blocks prepared by a modified Ogawa protocol (see the Supporting Information).^[32a,47]

The isothiocyanate linker **39** was obtained in 72% yield from the corresponding alcohol **17b**^[40] by an original and straightforward conversion of the alcohol group to azide and subsequent conversion of the azido group into the isothiocyanate functionality by treating the crude intermediate with carbon disulfide (Scheme 2A). The conversion of the primary alcohol into the azide group was achieved by a modification of the described procedure (sodium azide and triphenylphosphine in CCl_4/DMF),^[48] replacing tetrachloromethane with bromotrichloromethane.^[49]

The isothiocyanate-functionalized linker **39** was coupled to the monomannoside **27**, dimannoside **28**, and tetramannoside **30** in the presence of triethylamine in methanol (Scheme 2B) to obtain the neoglycoconjugates as thioacetyl

derivatives. Purification on silica gel resulted in low yields of the disaccharide derivatives. Sephadex LH-20 was thus used for purification of the thioacetyl-protected neoglycoconjugates. The monosaccharide **33**, the disaccharide **34**, and the tetrasaccharide **36** glycoconjugates were obtained after methanolysis in yields of 81, 73, and 81% (referred to two steps), respectively. Trimannoside **29**, pentamannoside **31**, and heptamannoside **32** were coupled to the isothiocyanate linker **39** using triethylamine in water/isopropanol/acetonitrile (1:1:1) as no reaction occurred in methanol. Evaporation of the solvents, trituration of the crude product with diethyl ether until complete removal of the unreacted linker, and desalting of the mixture and elimination of unreacted aminosugar by chromatography on Sephadex LH-20 furnished the pure thioacetyl derivatives. Deprotection of the thioacetyl group afforded the corresponding neoglycoconjugates **35**, **37**, and **38** in yields of 72, 73, and 52% (referred to two steps), respectively. The described reaction conditions were successfully ap-

plied to each of the aminoethyl mannosides **27–32** to furnish products **33–38** in good yields.

Preparation of glyconanoparticles: Three types of *manno*-GNPs (**1–3**, **4–7**, and **8–13**; Figure 1) were prepared and characterized by the procedure developed in our laboratory.^[5,27] An aqueous solution of tetrachloroauric acid was added to a methanolic solution of the neoglycoconjugate or to a mixture of variable proportions of glycoconjugates and stealth component. The resulting mixture was reduced with an excess of NaBH_4 and the suspension was vigorously shaken for 2 h at 25°C. The supernatant was removed and the residue was dissolved in milliQ water, purified by dialysis or centrifugal filtration, and characterized by ^1H NMR spectrometry, transmission electron microscopy (TEM), and ultraviolet spectroscopy (UV) (Figure 3). Glyconanoparticles with 100% density (**1–3**, **8**, and **9**) or variable density of sugars (**3a–c**, **4–7**, **9a,b**, **10a,b**, **11a,b**, **12a,b**, and **13a**) were obtained by controlling the ratio of neoglycoconjugate to stealth component (GlcC_2S , GlcC_5S , or mixed linker **40**) in the initial aqueous solution. The proportion of the ligands on the gold surface was examined by ^1H NMR before and after cluster formation (Figure 3C). GNPs functionalized with 100% glucose ($\text{GlcC}_5\text{-Au}$), lactose (*lacto* $\text{EG}_6\text{C}_{11}\text{-Au}$), or mixed linker ($\text{HO}_2\text{C-Au}$) (Figure 1D) were also prepared as control systems.

The resulting GNPs showed an exceptionally small core (1–2 nm), as demonstrated by TEM analysis. TEM micro-

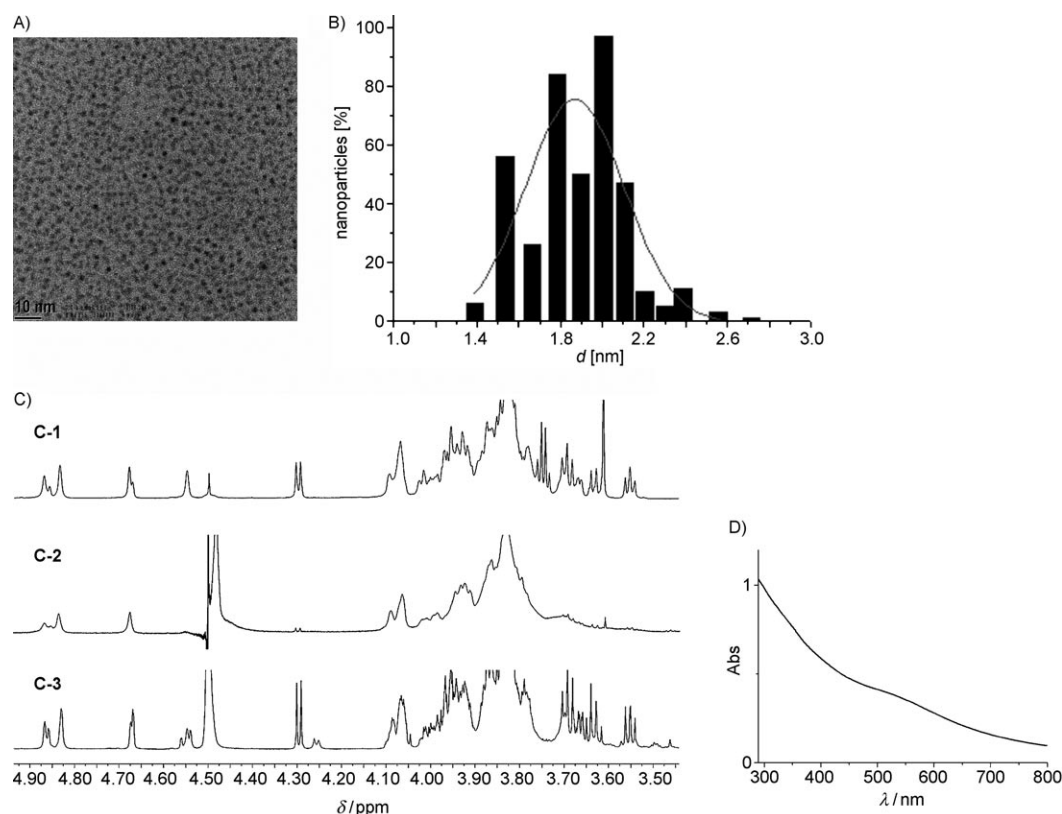


Figure 3. Characterization of glyconanoparticles **11a**: A) TEM micrograph in H₂O; B) size-distribution histogram; C) ¹H NMR spectra of mixtures of neoglycoconjugates GlcC₅S and tetramannoside **36** before (C-1) and after (C-3) GNP formation, and of the corresponding GNP **11a** (C-2); D) UV/Vis spectrum.

graphs showed uniform dispersion of the GNPs and no aggregation was evident. The UV/Vis spectra were often characterized by a surface plasmon band at around 520 nm, except in the case of the smallest core-sized GNPs, for which the plasmon was scarcely visible. The ¹H NMR spectra of the GNPs featured broader peaks compared to those of the corresponding neoglycoconjugates. An example of GNP characterization is shown in Figure 3.

All of the GNPs were found to be water-soluble (although solubilization of the thiourea linkage-containing GNPs was slow), and were stable for months under physiological conditions without flocculation. Based on the gold core size (de-

termined by TEM) and elemental analysis, an average molecular formula was estimated (Table 1). Molecular weights (MW), calculated according to the literature,^[50] were in agreement with those obtained on the basis of elemental analyses.

Manno-glyconanoparticles as inhibitors of DC-SIGN binding to gp120: Glyconanoparticles (*manno*-GNPs) with different (oligo)mannoside motifs were tested as inhibitors of gp120 binding to DC-SIGN. (Oligo)mannosides mimicking carbohydrate structures on gp120 can inhibit DC-SIGN/gp120 binding by competitive interaction with DC-SIGN.

Table 1. Chemical properties of selected glyconanoparticles.

GNP	Mannoside	Average diameter of gold particles [nm]	Average number of gold atoms ^[a]	Average molecular formula	Average mannoside copy number	Average M_w ^[a]
4	Man α 1-2Man	1.3 ± 0.6	79	(C ₃₄ H ₇₂ NO ₁₈ S) ₂₅ (C ₂₃ H ₄₅ O ₈ S) ₁₃ Au ₇₉	25	43 398
5	Man α 1-3Man	1.0 ± 0.4	79	(C ₃₄ H ₇₂ NO ₁₈ S) ₁₉ (C ₂₃ H ₄₅ O ₈ S) ₁₉ Au ₇₉	19	41 376
6	Man α 1-3(Man α 1-2)Man	1.3 ± 0.5	79	(C ₄₄ H ₈₃ NO ₂₃ S) ₂₅ (C ₂₃ H ₄₅ O ₈ S) ₁₃ Au ₇₉	25	47 451
7	Man α 1-2Man α 1-2Man	1.3 ± 0.5	79	(C ₄₄ H ₈₃ NO ₂₃ S) ₁₉ (C ₂₃ H ₄₅ O ₈ S) ₁₉ Au ₇₉	19	44 190
9a	Man α 1-2Man	1.3 ± 0.4	79	(C ₃₄ H ₆₃ N ₂ O ₁₅ S ₂) ₂₂ (C ₁₁ H ₂₁ O ₆ S) ₂₂ Au ₇₉	22	39 482 ^[b]
9	Man α 1-2Man	1.2 ± 0.5	79	(C ₃₄ H ₆₃ N ₂ O ₁₅ S ₂) ₅₉ Au ₇₉	59	63 058 ^[b]
GlcC ₅ -Au	–	1.6 ± 0.4	140	(C ₁₁ H ₂₁ O ₆ S) ₃₅ Au ₁₄₀	–	37 422 ^[b]
HO ₂ C-Au	–	2.7 ± 0.5	586	(C ₂₃ H ₄₁ O ₈ S) ₁₃₅ Au ₅₈₆	–	179 903

[a] The average number of gold atoms in the cluster, the molecular formulae, and the molecular weights of the nanoparticles were calculated according to the average gold diameter obtained by TEM.^[50] [b] Values confirmed by elemental analysis.

Multivalent presentation of (oligo)saccharides on GNPs may significantly increase their inhibitory potency, thereby improving their potential as microbicides. SPR-based competitive assays have been used to evaluate selected *manno*-GNPs as inhibitors of DC-SIGN binding to gp120. SPR inhibition assays were carried out by direct immobilization of gp120 on the sensor chip surface and binding measurements of fluid-phase DC-SIGN at a fixed concentration in the presence of *manno*-GNPs or free alkyl amino (oligo)mannosides at varying stoichiometric ratios.

Free (oligo)mannosides, as well as *manno*-GNPs, showed dose-dependent inhibition of DC-SIGN binding to gp120. The inhibitory activity of free alkyl amino (oligo)mannosides was compared to that of methyl α -D-mannopyranoside. All of the free (oligo)mannosides, except for Man α 1-3Man α 1-6Man α and Man α 1-4Man α , completely inhibited the gp120/DC-SIGN interaction at concentrations in the 1–3 mM range. A higher concentration (25 mM) of α -methyl mannopyranoside was required for 100% inhibition. On an equimolar basis (500 μ M concentration), disaccharide **18** (90% inhibition) and trisaccharide **20** (85% inhibition) were the best inhibitors (data not shown). Man α 1-2Man α **18** was more effective than Man α 1-3Man α **19** (40% inhibition) or pentasaccharide GlcNAc β 1-2Man α 1-3(GlcNAc β 1-2Man α 1-6)Man α (GlcNAc $_2$ Man $_3$) (64% inhibition), confirming a preference of DC-SIGN for a terminal α 1 \rightarrow 2 linkage^[51] and suggesting that a higher complexity of the oligosaccharide does not enhance inhibitory activity. Disaccharide Man α 1-2Man α **18** was able to fully inhibit the interaction at a concentration of 2.2 mM. We then asked whether the potency of the free (oligo)mannosides could be boosted by presentation in a multivalent display on a gold surface. GNPs **1**, **2**, **3**, and **3a–c**, coated with mannose monosaccharide at variable densities (Figure 1A), inhibited DC-SIGN/gp120 binding (100%) at 20 μ M (data not shown), which is at least 1000-fold lower than the concentration of methyl α -D-mannopyranoside required to observe complete inhibition. Under similar experimental conditions, a glycodendrimer with 32 mannose units inhibited 50% of the binding at sub-millimolar concentrations.^[26] Glucose-GNP (GlcC $_5$ -Au) and lactose-GNP (*lacto*EG $_6$ C $_{11}$ -Au) showed no inhibitory activity at concentrations as high as 50 μ M, and were used as negative controls.

GNPs **4–6**, containing Man α 1-2Man α , Man α 1-3Man α , or Man α 1-2Man α 1-2Man α and carboxyl linker **40** at different densities, fully inhibited binding at concentrations between 0.115 and 4.3 μ M on the GNP. In particular, multivalent presentation of Man α 1-2Man α on GNP **4**, characterized by 25 units of disaccharide Man α 1-2Man α and an average molecular weight of \sim 43 kDa, resulted in 20 000-fold increased activity (100% inhibition at 115 nM) compared to the corresponding monomeric disaccharide **18** (100% inhibition at 2.2 mM) (Figure 4). The level of inhibition (approximately 50%) upon co-injection with 6 nM GNP **4** suggests binding of more than one molecule of DC-SIGN per particle.

GNP **4** was also more potent than Man α 1-2Man α 1-2Man α -GNP **6** and Man α 1-3Man α -GNP **5**, which displayed

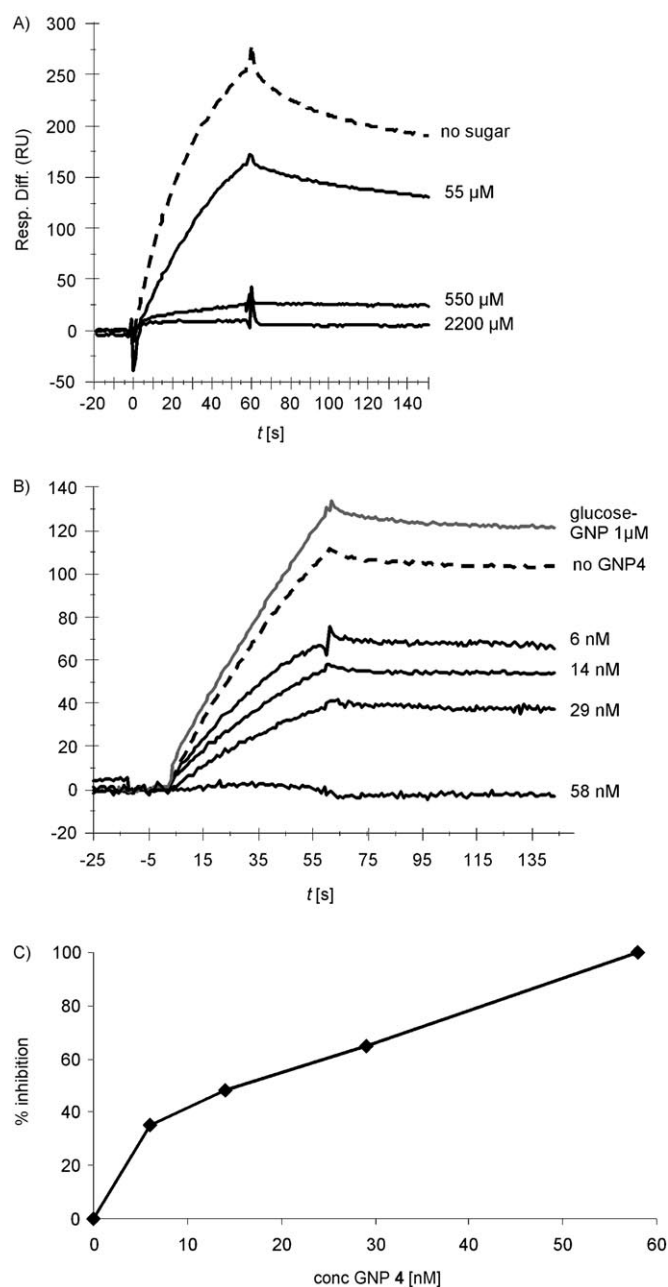


Figure 4. Inhibitory activity of Man α 1-2Man versus Man α 1-2Man-coated GNP **4**. gp120(CN54) was immobilized by direct amine coupling (\sim 1000 resonance units (RU)). The binding activity of fluid-phase DC-SIGN in the presence of free Man α 1-2Man α (A) was determined and compared to that of DC-SIGN in the presence of Man α 1-2Man α -coated GNP **4** (B). A) Superimposed sensorgrams representing DC-SIGN (100 nM) binding activity in the absence (dotted curve) and presence (solid curves) of Man α 1-2Man α at (55–2200 μ M). B) Dose-dependent gp120/DC-SIGN binding inhibition by GNP **4**. DC-SIGN (50 nM) binding in the presence of **4** (6–115 nM) compared to that in the presence of GlcC $_5$ S-Au at 1 μ M (grey curve) and in the absence of inhibitor (dotted curve). Sensorgrams shown in this panel were obtained by subtraction of the sensorgram obtained following injection of GNPs alone from that generated by injection of GNPs in the presence of DC-SIGN. The buffer used was HBS-P supplemented with 10 mM CaCl $_2$. The flow rate was 20 μ Lmin $^{-1}$ and the injection volume was 20 μ L. C) Plot of the data from B) showing % inhibition at each concentration.

full inhibitory activity at 1.2 μM and 4.3 μM , respectively. The presence of an additional mannose unit in position 2 did not improve the inhibitory activity of the nanoparticle. These findings support the data of the experiments with free alkyl-amino (oligo)mannosides, which showed that the complexity of the mannoside structures does not enhance the inhibitory activity of the compound and that $\text{Man}\alpha 1\text{-}2\text{Man}\alpha$ structures are more effective inhibitors. Table 2 summarizes the inhibitory activity of selected glyconanoparticles (data analysis of the best-fit curves and estimated IC_{50} and IC_{90} values are reported in the Supporting Information; Figure S5 and Table S1).

Table 2. *Manno*-GNPs as inhibitors of DC-SIGN-ECD binding to immobilized gp120.

GNP	Mannoside	Average man-nose copy number	$[\text{C}_{100}]^{[a]}/\mu\text{M}$	
			per GNP	per manno-side
4	$\text{Man}\alpha 1\text{-}2\text{Man}\alpha$	25	0.115	2.9
5	$\text{Man}\alpha 1\text{-}3\text{Man}\alpha$	19	4.3	82
6	$\text{Man}\alpha 1\text{-}2\text{Man}\alpha 1\text{-}2\text{Man}\alpha$	25	1.2	30
9	$\text{Man}\alpha 1\text{-}2\text{Man}\alpha$	59	0.08	4.7
9a	$\text{Man}\alpha 1\text{-}2\text{Man}\alpha$	22	0.13	2.9

[a] The nanoparticle concentration required to inhibit DC-SIGN-ECD binding to gp120 by 100%. Data shown are based on single measurements.

To confirm that inhibition mediated by GNPs occurs by direct interaction with DC-SIGN, GNP 4 binding activity to immobilized DC-SIGN-ECD was demonstrated. Sensorgrams representing GNP 4 binding at various concentrations (0.25–2 μM) were fitted to the linked-reaction model with a K_D value of $9.74 \times 10^{-7} \text{ M}$ (Figure 5). The surface of GNP 4 is partially (66%) coated with $\text{Man}\alpha 1\text{-}2\text{Man}\alpha$ neoglycoconjugate, and the remaining sites are occupied by COOH-terminated linkers. To determine whether the COOH groups contribute to GNP interaction with DC-SIGN, GNP $\text{HO}_2\text{C-Au}$ containing only COOH linker 40 was tested. No significant binding activity to DC-SIGN was detected (dotted curve, Figure 5A). Likewise, $\text{HO}_2\text{C-Au}$ did not exert any inhibitory effect at concentrations required to observe inhibition by GNP 4 (data not shown).

The binding affinity of DC-SIGN to a GNP containing 100% $\text{Man}\alpha 1\text{-}2\text{Man}\alpha$ -glycoconjugate (GNP 9) was approximately twofold higher than that observed for GNP 4 (Figure 5B) with faster on rates and slower k_{off} , although the overall level of binding was similar. GNP 9 inhibitory activity on the gp120/DC-SIGN interaction was also comparable to that exhibited by GNP 4 (data not shown). This suggests that a higher density of glycoconjugates does not improve the efficacy of the GNPs.

In experiments in which fluid-phase GNPs alone were injected on immobilized gp120, unexpected behaviour was observed. Most GNPs, including *gluco*-GNPs and nanoparticle $\text{HO}_2\text{C-Au}$, harbouring only the carboxylic linker, bound

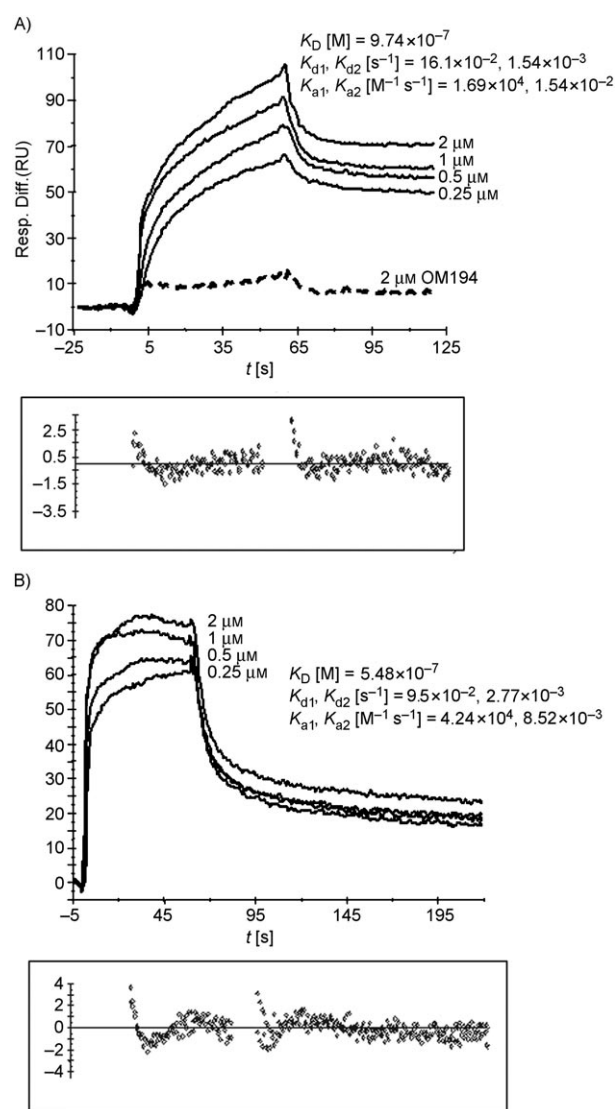


Figure 5. Effect of density of $\text{Man}\alpha 1\text{-}2\text{Man}$ neoglycoconjugates on GNP binding affinity to DC-SIGN. DC-SIGN-ECD (700 RU) was immobilized directly on the sensor chip surface. Binding of fluid-phase GNPs at 0.25–2 μM was then determined. A) Superimposed sensorgrams representing binding activity of GNP 4 (66% in $\text{Man}\alpha 1\text{-}2\text{Man}$) (solid curves) at varying concentrations to DC-SIGN. The $\text{HO}_2\text{C-Au}$ GNP at 2 μM (dotted curve) did not exhibit any binding activity. B) Sensorgrams showing GNP 9 (100% in $\text{Man}\alpha 1\text{-}2\text{Man}$) binding activity to immobilized DC-SIGN. Kinetic values estimated by fitting the sensorgrams to the linked reaction model are indicated. The buffer used was HBS-P supplemented with 10 mM CaCl_2 . The flow rate was $20 \mu\text{L min}^{-1}$ and the injection volume was 20 μL . Plots showing the deviation of data points from the fit (residuals) are shown below each sensorgram.

gp120 in a dose-dependent manner with affinity in the sub-micromolar range ($K_D \approx 10^{-8}\text{-}10^{-10} \text{ M}$) (data not shown). GNP 4 (0.1–1.0 μM) showed the strongest binding affinity, with a K_D value of the order of 10^{-11} M (see the Supporting Information, Figure S4A). SPR analysis suggested that GNP 4 and DC-SIGN do not share binding sites on gp120 (Figure S4B). The binding activities of dimannose- and glucose-

coated GNPs to gp120 are difficult to interpret. Carbohydrate–protein interactions or Ca^{2+} -mediated carbohydrate–carbohydrate interactions may be the basis of this effect. Lectin-binding has been described for gp41^[52] but not for gp120. Because gp120 is heavily glycosylated, gp120 interaction with *manno*-GNPs could be of the carbohydrate–carbohydrate type, as shown for Lewis X-coated GNPs^[4,7] and proposed for the interaction of integrin $\alpha_5\beta_1$ with glycosphingolipids.^[52,53] Binding to gp120 by nanoparticles bearing carboxylic acid groups can also be explained in terms of electrostatic interactions with positively charged surfaces of the glycoprotein.^[54] Non-specific binding activity by the gold core can be ruled out as GNPs **1** fully functionalized with the short linker conjugate ManC₂S did not show significant binding to gp120 (Figure S4A).

Because *manno*-GNPs can be used as potential microbicides that block the binding of HIV and other pathogens to DC-SIGN-expressing cells and thus prevent infection,^[24,55] we are now investigating their cytotoxicity and their potency as inhibitors of DC-SIGN-mediated HIV-1 trans-infection in human T cells.

Conclusions

In summary, we have reported the synthesis and characterization of a small library of (oligo)mannose glyconanoparticles (*manno*-GNPs) incorporating diverse neoglycoconjugates synthesized either by direct glycosylation (first family: GNPs **1–3** and **3a–c**), by peptide linkage (second family: GNPs **4–7**), or by thiourea linkage (third family: GNPs **8, 9, 9a,b, 10a,b, 11a,b, 12a,b, and 13a**). The thiourea strategy proved to be the most efficient in terms of yields and versatility of the synthetic procedure. The generated GNPs have been tested by SPR for competitive inhibition of DC-SIGN/gp120 binding. The results of this study have allowed us to identify the best inhibitor among these new biocompatible 3D systems and have confirmed a multivalent effect of the mannosides on the gold surface compared with the corresponding monomer conjugates. The Man α 1-2Man α -containing GNPs were found to be the best inhibitors, with inhibition values in the nanomolar range. In this study, changing the density of Man α 1-2Man α on GNPs from 50 % to 100 % did not improve the inhibitory activity. Values are in agreement with those reported for more complex (oligo)mannose clusters and dendrimers.^[25,26] The gold clusters offer a rigid scaffold, the size of which can be varied. As has been shown, the glyconanoparticle technology allows the selection of length and flexibility of the linkers as well as sugar density for improved presentation of the (oligo)mannosides. Furthermore, by means of glyconanotechnology, the GNPs platform can be simultaneously tailored with different biologically-relevant molecules (such as immunogenic peptides or other antigens),^[27] thereby allowing the preparation of multifunctional structures as potential carbohydrate-based systems against HIV.^[56]

Experimental Section

General procedures: All chemicals were purchased as reagent grade from Sigma–Aldrich, except chloroauric acid (Strem Chemicals), and were used without further purification. Aminopropyl mannosides **18–21** were provided by Carbohydrate Synthesis Ltd. Reactions were monitored by thin-layer chromatography (TLC) on silica gel 60 F₂₅₄ aluminium-backed sheets (Merck) with visualization under UV (254 nm) and/or by staining with *p*-anisaldehyde solution [anisaldehyde (25 mL), H₂SO₄ (25 mL), EtOH (450 mL), and CH₃COOH (1 mL)], 10% H₂SO₄ solution in EtOH, ninhydrin solution [ninhydrin (0.25 mL), EtOH (100 mL)] or phosphomolybdic acid solution [phosphomolybdic acid (13 g), Ce(SO₄)₂ (10 g), H₂SO₄ (60 mL), H₂O (940 mL)] followed by heating at over 200 °C. Size-exclusion column chromatography was performed on Sephadex LH-20 (GE Healthcare). Flash column chromatography (FCC) was performed on silica gel 60 (0.063–0.200 mm or 0.015–0.040 mm; Merck). UV/Vis spectra were measured with Perkin–Elmer Lambda 12 or Beckman Coulter DU 800 UV/Vis spectrophotometers. Infrared (IR) spectra were recorded from 4000 to 750 cm⁻¹ with a JASCO FT-IR 410 model spectrometer; solids were pressed into KBr pellets and oils were subjected to attenuated total reflection (ATR). ¹H and ¹³C NMR spectra were recorded on Bruker DPX-300 (300 MHz) or Bruker AVANCE (500 MHz) spectrometers. Chemical shifts (δ) are given in ppm relative to the residual signal of the solvent used. Coupling constants (*J*) are reported in Hz. Splitting patterns are described by using the following abbreviations: br, broad; s, singlet; d, doublet; t, triplet; m, multiplet. Mass spectra were measured with an Esquire 6000 ESI-Ion Trap spectrometer from Bruker Daltonics. High-resolution mass spectra (HRMS) were obtained using the MALDI technique with a 4700 Proteomics Analyzer (Applied Biosystems) operated in MALDI-TOF-TOF configuration. Samples of the products were dissolved in water, 2,5-dihydroxybenzoic acid (DHB) was used as a matrix, cesium iodide was added to favour the ionization process, and polyethylene glycol was used as an internal reference. Optical rotations were determined with a Perkin–Elmer 341 polarimeter. For transmission electron microscopy (TEM) examinations, a single drop (10 μ L) of an aqueous solution (ca. 0.1 mg mL⁻¹ in Milli-Q water) of the gold glyconanoparticles (GNPs) was placed on a copper grid coated with a carbon film (Electron Microscopy Sciences). The grid was left to dry in air for several hours at room temperature. TEM analysis was performed with a Philips CM200 or a Philips JEOL JEM-2100F microscope, both operating at 200 kV. The average diameters and numbers of gold atoms of the GNPs were deduced as described in a previous study.^[50] Laboratory distilled water was further purified using a Milli-Q reagent grade water system (Millipore).

Recombinant proteins: gp120 from HIV-1 strain CN54 (clade C) was produced using the baculovirus system and was kindly provided by Ian Jones (University of Reading, Reading, UK). The full-length extracellular domain of DC-SIGN (DC-SIGN-ECD) was expressed and purified as follows: cDNA of iMDDC was used as a template to generate the DNA fragment encoding the entire extracellular domain of DC-SIGN (residues 70–404; GenBank accession number NP 066978) by PCR with primers 5'-GTCTCGAGATGGAAACAATCCAGGCAAGACGCGATCT-3' (sense) and 5'-TCGGATCCCTACGCAGGAGGGGGTTTGGGGT-3' (antisense). The amplified sequence, digested with XhoI and BamHI, was inserted into pET15b (Novagen, EMD Chemicals, Gibbstown, NJ, USA) and cloned in *E. coli* TOP10 (Invitrogen, Paisley, UK). Cloned fragments were confirmed by DNA sequencing (Advanced Biotechnology Centre, Imperial College London, London, UK) and compared with GenBank (accession number NM_021155). For expression, *E. coli* strain BL21/DE3 (Stratagene, La Jolla, CA, USA) was transformed with recombinant plasmid. Protein expression and refolding was performed as described elsewhere^[57] with minor modifications. Inclusion bodies (from 1 L bacterial culture) were recovered by centrifugation at 10000 \times g for 20 min at 4 °C and solubilized in 8 mL of 100 mM Tris-HCl, pH 8.0, containing 6 M urea (solubilizing buffer) supplemented with 0.01 % 2-mercaptoethanol, by gentle rotation overnight at 4 °C. The mixture was centrifuged at 20000 \times g for 30 min at 4 °C and soluble recombinant protein was isolated by Ni²⁺-affinity chromatography. Bound material (recovered by elution with

200 mM imidazole in solubilizing buffer) was dialyzed against 2 L of 100 mM Tris-HCl, pH 8.0, containing 0.01% 2-mercaptoethanol, 10 mM CaCl₂, and 6 M urea, then successively against the same buffer with 4 M urea, 2 M urea, and no urea. Final dialysis was against 100 mM Tris-HCl, pH 8.0, containing 10 mM CaCl₂. After dialysis, the insoluble precipitate was removed by centrifugation at 100000 × *g* for 30 min at 4 °C and re-folded DC-SIGN contained in the soluble fraction was purified by D-mannose affinity chromatography as previously described.^[58] Fractions were analyzed by SDS-PAGE and protein concentrations were determined by densitometric analysis using the GeneSnap software (Syngene, Cambridge, UK). The identity of the protein was confirmed by LC MS/MS analysis (MRC Clinical Sciences Centre, Imperial College London, London, UK).

Surface plasmon resonance assays

Inhibition studies: gp120 in 10 mM sodium acetate at pH 4.0 was immobilized (approximately 1000 RU, which corresponds to ~1 ng of immobilized ligand on a CM5 sensor chip)^[59] on the surface of Flow cell 2 of a CM5 sensor chip following the standard amine coupling procedure (GE Healthcare, Uppsala, Sweden). Flow cell 1 (activated and blocked with ethanolamine) served as a reference (blank) cell. Non-saturation binding concentrations of DC-SIGN were chosen to increase the sensitivity of the inhibition assay. Binding of fluid-phase DC-SIGN-ECD at a concentration of 50 nM was determined in the presence of free alkyl amino (oligo)-mannosides (0.01–3 mM), methyl α-D-mannopyranoside (0.5–25 mM, Sigma–Aldrich), or GNPs and compared to the binding activity of DC-SIGN-ECD alone. GNPs **1**, **2**, **3**, and **3a** were tested at concentrations in the range 0.5–20 μM. For GNPs **5** and **6**, concentrations were varied in the range 0.1–2.0 μM. GNPs **4**, **9**, and **9a** were tested at 6–130 nM. GlcC₅Au and HO₂C–Au GNPs were tested at 1 μM and 2 μM, respectively. For GNPs that showed direct binding activity to gp120, final inhibition sensorgrams were obtained by subtraction of the sensorgram for injection of GNPs alone from that generated by injection of GNPs in the presence of DC-SIGN. Fluid-phase compounds were dissolved in HBS-P buffer (10 mM HEPES [pH 7.4], 0.15 M NaCl, 0.005% v/v surfactant P20; GE Healthcare) supplemented with 10 mM CaCl₂. The flow rate was 20 μL min⁻¹ and the injection volume was 20 μL. After each binding measurement, the surface was regenerated with 10 mM EDTA. Single measurements were carried out for each condition.

Affinity measurements: DC-SIGN-ECD (500–700 RU) or gp120 (approximately 500 RU) were immobilized in Flow cell 2 on a CM5 sensor chip as described above. In both cases, Flow cell 1, treated as above, served as a reference cell. Binding of fluid-phase GNPs was determined over a range of concentrations (2.3–10.7 μM when determining binding to DC-SIGN, 0.01–5.0 μM when determining binding to gp120) in HBS-P supplemented with 10 mM CaCl₂. GlcC₅Au and HO₂C–Au GNPs were tested at concentrations as high as 2 μM. The injection volume was 20 μL and the flow rate was 20 μL min⁻¹. The surface was regenerated with 10 mM EDTA. Equilibrium dissociation constants (*K*_D) as well as association (*k*_a) and dissociation constant (*k*_d) rates were calculated using the BIA evaluation software 4.1 (GE Healthcare). Curves were first fitted to a single 1:1 binding model and then to more complex binding models, selecting that which gave the best fit as judged by the lowest χ² value and the best distribution of residuals.

General procedure for thiourea coupling

A solution of the respective aminoethyl (oligo)mannoside **27–32** (0.09 M, 1 equiv) in methanol (for **27**, **28**, and **30**) or H₂O/*i*PrOH/CH₃CN (1:1:1) (for **29**, **31**, and **32**) was added to a solution of isothiocyanate linker **39** (0.12 M, 2 equiv) in methanol or H₂O/*i*PrOH/CH₃CN (1:1:1), respectively. The pH was adjusted to 8–9 with triethylamine and the solution was stirred for 3–5 h at room temperature. The solvent was then removed under reduced pressure and the crude residue was triturated with Et₂O to remove the excess linker (except in the case of the neoglycoconjugate of **27**). The resulting thioacetyl derivatives were purified by FCC or on Sephadex LH-20 (for complete characterization of these intermediates, see the Supporting Information). The thioacetyl derivatives were treated with sodium methoxide (1 equiv, 1 N in MeOH). The resulting mixture was stirred for 2 h at room temperature and then neutralized with 0.1 N HCl. Purification on a column of Sephadex LH-20 followed by lyophilization

afforded the glycoconjugates **33–38**. For the sake of clarity, these neoglycoconjugates are all named as their disulfides. The thiol/disulfide ratio is reported in each case on the basis of the integrals of the relevant signals in the corresponding ¹H NMR spectra.

23,23'-Dithiobis[*N*-(ethyl α-D-mannopyranosyl),*N'*-(3,6,9,12-tetraoxa-tricosanyl)thiourea] (33**):** Reaction of mannoside **27** (50.0 mg, 0.224 mmol) and linker **39** (207.7 mg, 0.448 mmol) afforded neoglycoconjugate **33** in the form of the disulfide (117.4 mg, 0.182 mmol, 81% over two steps) as a colourless syrup after purification by passage through Sephadex LH-20 (CH₂Cl₂/MeOH 4:1). ¹H NMR (300 MHz, CD₃OD): δ = 4.78 (s, 1H; 1-H), 3.90–3.51 (m, 26H), 3.47 (t, *J* = 6.6 Hz, 2H; OCH₂CH₂CH₂), 2.69 (t, *J* = 6.9 Hz, 2H; CH₂SS), 1.72–1.64 (m, 2H), 1.61–1.53 (m, 2H), 1.47–1.20 ppm (m, 14H); ¹³C NMR (75 MHz, CD₃OD): δ = 101.8 (d; C-1), 74.8, 72.6, 72.4, 72.1, 71.6, 71.4, 71.2, 70.7, 68.6, 67.4 (t; NHCH₂CH₂O), 62.9 (t; C-6), 45.3 (brt; CH₂NHCS), 39.9 (t; CH₂SS), 30.8, 30.7, 30.6, 30.36, 30.27, 29.5, 27.3 ppm; C=S undetected; IR (neat): ν̄ = 3331 (brs), 2924, 2854, 1647, 1560, 1458, 1348, 1294, 1097 cm⁻¹; HRMS: *m/z*: calcd for C₂₈H₅₆N₂O₁₀S₂Na⁺ [*M*+Na]⁺: 667.3274; found: 667.3273.

23,23'-Dithiobis[*N*-(ethyl α-D-mannopyranosyl-(1→2)-α-D-mannopyranosyl),*N'*-(3,6,9,12-tetraoxa-tricosanyl)thiourea] (34**):** Reaction of mannoside **28** (25.0 mg, 0.065 mmol) and linker **39** (60.1 mg, 0.130 mmol) afforded neoglycoconjugate **34** in the form of the disulfide (38.3 mg, 0.047 mmol, 73% over two steps) as a colourless syrup after purification by passage through Sephadex LH-20 (MeOH/H₂O 9:1). ¹H NMR (500 MHz, CD₃OD): δ = 5.11 (d, *J* = 1.5 Hz, 1H; 1-H), 4.97 (d, *J* = 1.5 Hz, 1H; 1'-H), 3.98–3.96 (m, 1H; 2'-H), 3.90–3.80 (m, 5H), 3.75–3.50 (m, 26H), 3.47 (t, *J* = 6.5 Hz, 2H; OCH₂CH₂CH₂), 2.69 (t, *J* = 7 Hz, 2H; CH₂SS), 1.72–1.63 (m, 2H), 1.61–1.53 (m, 2H), 1.44–1.28 ppm (m, 14H); ¹³C NMR (125 MHz, D₂O): δ = 104.2 (d; C-1), 100.1 (d; C-1'), 80.5 (d; C-2), 75.1, 74.8, 72.4, 72.1, 71.9, 71.6, 71.3, 71.1, 70.7, 69.0, 68.8, 67.4, 63.2, and 63.0 (t, 2C; C-6 and C-6'), 45.3 (brt; CH₂NH₂), 39.8 (t; CH₂SS), 30.7, 30.6, 30.6, 30.3, 30.2, 29.4, 29.4, 27.2 ppm; C=S undetected; IR (neat): ν̄ = 3330 (brs), 2923, 2853, 1645, 1556, 1456, 1348, 1297, 1057 cm⁻¹; HRMS: *m/z*: calcd for C₃₄H₆₆N₂O₁₅S₂Na⁺ [*M*+Na]⁺: 829.3802; found: 829.3802.

23,23'-Dithiobis[*N*-(ethyl α-D-mannopyranosyl-(1→2)-α-D-mannopyranosyl-(1→2)-α-D-mannopyranosyl),*N'*-(3,6,9,12-tetraoxa-tricosanyl)thiourea] (35**):** Reaction of the formate salt of mannoside **29** (21.4 mg, 0.036 mmol) and linker **39** (33.0 mg, 0.071 mmol) afforded neoglycoconjugate **35** (24.4 mg, 0.025 mmol, 72% over two steps) as a white solid after purification by passage through Sephadex LH-20 (MeOH/H₂O 9:1). ¹H NMR (500 MHz, CD₃OD): δ = 5.28 (d, *J* = 1.5 Hz, 1H; 1-H), 5.10 (d, *J* = 1.5 Hz, 1H; 1'-H), 4.98 (d, *J* = 1.5 Hz, 1H; 1''-H), 4.05–4.02 (m, 1H; 2-H), 3.99–3.95 (m, 1H; 2''-H), 3.89–3.80 (m, 6H), 3.76–3.50 (m, 30H), 3.47 (t, *J* = 6.5 Hz, 2H; OCH₂CH₂CH₂), 2.69 (t, *J* = 7.0 Hz, 0.3H; CH₂SS), 2.49 (t, *J* = 7.5 Hz, 1.7H; CH₂SH), 1.63–1.53 (m, 4H), 1.45–1.35 ppm (m, 14H); ¹³C NMR (125 MHz, CD₃OD): δ = 104.1 (d; C-1'), 102.5 (d; C-1), 100.0 (d; C-1'), 80.6 (d; C-2'), 80.2 (d; C-2), 75.02, 75.00, 74.7, 72.43, 72.40, 72.0, 71.92, 71.87, 71.5, 71.3, 71.1, 70.7, 69.2, 69.0, 68.8, 67.4; 63.3, 63.2, and 62.9 (t, 3C; 3 × C-6), 45.2 (brt; CH₂NH), 35.2 (t; CH₂SS), 30.69, 30.63, 30.5, 30.2, 29.4, 27.2, 25.0 ppm (t; CH₂SH); C=S undetected; HRMS: *m/z*: calcd for C₄₀H₇₆N₂O₂₀S₂Na⁺ [*M*+Na]⁺: 991.4331; found: 991.4330.

23,23'-Dithiobis[*N*-(ethyl α-D-mannopyranosyl-(1→2)-α-D-mannopyranosyl-(1→2)-α-D-mannopyranosyl-(1→3)-α-D-mannopyranosyl),*N'*-(3,6,9,12-tetraoxa-tricosanyl)thiourea] (36**):** Reaction of mannoside **30** (63.0 mg, 0.0874 mmol) and linker **39** (81.0 mg, 0.175 mmol) afforded neoglycoconjugate **36** (80.0 mg, 0.071 mmol, 81% over two steps) as a white solid after passage through Sephadex LH-20 (MeOH/H₂O 9:1). ¹H NMR (500 MHz, D₂O): δ = 5.38 (s, 1H), 5.32 (s, 1H), 5.07 (s, 1H), 4.87 (s, 1H), 4.13–3.59 (m, 44H), 3.51 (brt, 2H; OCH₂CH₂CH₂), 2.73 (t, *J* = 7.1 Hz, 2H; CH₂SS), 1.78–1.56 (m, 4H), 1.49–1.28 ppm (m, 14H); ¹³C NMR (125 MHz, D₂O): δ = 102.2, 100.62 (overlapped), 99.7, 78.4, 78.1, 73.3, 73.23, 73.17, 72.9, 71.2, 70.3, 70.0, 69.9, 69.7, 69.2, 66.9, 66.8, 65.9, 61.0, 60.9, 60.7, 43.7 (brt; CH₂NH), 39.0, 34.1, 29.7, 29.6, 29.5, 29.3, 28.5, 26.1 ppm; C=S undetected; IR (KBr): ν̄ = 3361 (broad), 2926, 2856, 1646, 1556, 1459, 1352, 1296, 1131, 1058 cm⁻¹; HRMS: *m/z*: calcd for C₄₆H₈₆N₂O₂₅S₂Na⁺ [*M*+Na]⁺: 1153.4859; found: 1153.4879.

23,23'-Dithiobis[*N*-(ethyl (bis(α-D-mannopyranosyl-(1→2)-α-D-mannopyranosyl-(1→3,6))-α-D-mannopyranosyl)),*N'*-(3,6,9,12-tetraoxa-trico-

nyl)thiourea] (37): Reaction of the formate salt of mannoside **31** (18.9 mg, 0.0206 mmol) and linker **39** (19.1 mg, 0.041 mmol) afforded neoglycoconjugate **37** (19.4 mg, 0.015 mmol, 73% over two steps) as a white solid after purification by passage through Sephadex LH-20 (MeOH/H₂O 5:1). ¹H NMR (D₂O, 500 MHz): δ = 5.38 (s, 1H), 5.16 (s, 1H), 5.08 (s, 1H), 5.06 (s, 1H), 4.86 (s, 1H), 4.16–3.60 (m, 50H), 3.52 (brt, 2H; OCH₂CH₂CH₂), 2.73 (brt, 0.7H; CH₂SS), 2.55 (t, 1.3H, *J* = 6.9 Hz; CH₂SH); 1.80–1.56 (m, 4H), 1.49–1.26 ppm (m, 14H); ¹³C NMR (D₂O, 125 MHz): δ = 102.3, 102.3, 100.7, 100.0, 98.0, 78.7, 78.4, 73.2, 72.7, 72.0, 71.1, 70.8, 70.4, 70.3, 69.9, 69.7, 69.2, 69.1, 66.9, 66.7, 65.9, 65.6, 65.3, 61.1, 60.9, 43.7 (brt, 2C; OCH₂CH₂N), 39.0 (t; CH₂SS), 34.0, 29.72, 29.69, 29.5, 29.4, 29.2, 28.4, 26.1, 26.0, 24.3 ppm (t; CH₂SH); C=S undetected; IR (KBr): $\tilde{\nu}$ = 3386 (broad), 2926, 2854, 1642, 1556, 1462, 1366, 1301, 1131, 1057 cm⁻¹; HRMS: *m/z*: calcd for C₅₂H₉₆N₂O₃₀S₂Na⁺ [*M*+Na]⁺: 1315.5382; found: 1315.5380.

23,23'-Dithiobis[N-(ethyl (bis(α-D-mannopyranosyl-(1→2)-α-D-mannopyranosyl-(1→2)-α-D-mannopyranosyl-(1→3,6))-α-D-mannopyranosyl)-N'-(3,6,9,12-tetraoxatricosanyl)thiourea] (38): Reaction of the formate salt of mannoside **32** (17.2 mg, 0.0138 mmol) and linker **39** (12.8 mg, 0.0276 mmol) afforded neoglycoconjugate **38** (12.1 mg, 0.0075 mmol, 52% over two steps) as a white solid after purification by passage through Sephadex LH-20 (MeOH/H₂O 5:1). ¹H NMR (500 MHz, CD₃OD): δ = 5.37 (s, 1H), 5.32 (s, 1H), 5.32 (s, 1H), 5.13 (s, 1H), 5.07 (s, 1H), 5.07 (s, 1H), 4.86 (s, 1H), 4.14–3.63 (m, 62H), 3.52 (brt, 2H; OCH₂CH₂CH₂), 2.73 (brt, 1.1H; CH₂SS), 2.56 (t, 0.9H, *J* = 6.9 Hz, CH₂SH), 1.79–1.56 (m, 4H), 1.49–1.25 ppm (m, 14H); ¹³C NMR (D₂O, 125 MHz): δ = 102.2, 102.2, 100.6, 100.6, 100.6, 100.0, 98.0, 78.5, 78.4, 73.2, 72.7, 71.3, 71.2, 70.3, 69.9, 69.7, 67.0, 66.9, 66.8, 61.0, 43.9 (brt, 2C; OCH₂CH₂N), 38.8 (t; CH₂SS), 29.8, 29.7, 29.5, 29.4, 29.3, 28.6, 26.1, 24.1 ppm (t; CH₂SH); C=S undetected; IR (KBr): $\tilde{\nu}$ = 3395 (broad), 2926, 2854, 1644, 1565, 1463, 1369, 1302, 1131, 1054 cm⁻¹; HRMS: *m/z*: calcd for C₆₄H₁₁₆N₂O₄₀S₂Na⁺ [*M*+Na]⁺: 1639.6443; found: 1639.6440.

General procedure for preparation of glyconanoparticles

A 0.012 M (3 equiv) methanolic solution of the appropriate disulfide **14–16** and mixture **22–25'**, or a mixture of disulfide **16** or **33–38** in different ratios (5:95, 10:90, 15:85, 30:70, or 50:50) with conjugate GlcC₂S or GlcC₃S was added to a solution of tetrachloroauric acid (0.025 M, 1 equiv) in water. An aqueous solution of NaBH₄ (1 M, 22 equiv) was then added in four portions, with rapid shaking. The black suspension formed was shaken for an additional 2 h at 25°C and then the supernatant was removed and analysed. The residue was dissolved in the minimum volume of NANOPURE water and purified by dialysis. This solution was loaded into 5–10 cm segments of SnakeSkin pleated dialysis tubing (Pierce, 3500 MWCO), which were placed in a 3 L beaker of water. The contents of the beaker were stirred slowly, recharging with fresh distilled water every 3–4 h over the course of 72 h. The solution in the membrane was then lyophilized to afford the GNP. ¹H NMR spectra of the glycoconjugate mixtures used for the GNP synthesis and of the products recovered from the supernatant after GNP formation were recorded. The ratio of the ligands in the GNPs was confirmed through integration of the signals of the anomeric protons of the mannoside with respect to those of the anomeric protons of the glucoside. The particle size distribution of the gold nanoparticles was evaluated from several TEM micrographs by means of an automatic image analyser. The average diameter and number of gold atoms of the GNPs was assigned according to a previous work.^[50] The average molecular formula of the nanoparticles was calculated on the basis of the average diameter obtained by TEM and confirmed by elemental analysis.

ManC₂-Au (100%) (1): Reaction of **14** (45.0 mg, 0.187 mmol) with HAuCl₄ (1.38 mL, 0.025 M) and NaBH₄ (760 μL, 1 N) gave **1** (5.8 mg) as a dark-brown powder. TEM (average diameter and number of gold atoms): 2.0 ± 0.6 nm, 225; ¹H NMR (500 MHz, D₂O): δ = 4.95 (s, 1H; 1-H), 4.40–3.50 ppm (m, 10H); UV/Vis (H₂O, 0.1 mg mL⁻¹): λ = 520 nm (surface plasmon band); elemental analysis calcd (%) for (C₈H₁₅O₆S)₁₂₁Au₂₂₅ (73 kDa): C 15.87, H 2.50, S 5.30; found: C 15.89, H 3.00, S 5.12.

ManC₃-Au (100%) (2): Reaction of **15** (50.0 mg, 0.177 mmol) with HAuCl₄ (1.29 mL, 0.025 M) and NaBH₄ (686 μL, 1 N) gave **2** (3.6 mg) as a

dark-brown powder. TEM (average diameter and number of gold atoms): 1.6 ± 0.5 nm, 140; ¹H NMR (500 MHz, D₂O): δ = 4.70 (s, 1H; 1-H), 4.05–3.00 (m, 6H), 2.11–1.02 ppm (m, 8H); UV/Vis (H₂O, 0.1 mg mL⁻¹): λ = 530 nm (surface plasmon band); elemental analysis calcd (%) for (C₁₁H₂₂O₆S)₇₃Au₁₄₀ (48 kDa): C 20.01, H 3.36, S 4.86; found: C 20.16, H 3.22, S 4.70.

ManEG₆C₁₁-Au (100%) (3): Reaction of **16** (45.0 mg, 0.071 mmol) with HAuCl₄ (520 μL, 0.025 M) and NaBH₄ (686 μL, 1 N) gave **3** (1.2 mg) as a brown powder. TEM (average diameter and number of gold atoms): 1.0 ± 0.9 nm, 79; ¹H NMR (500 MHz, D₂O): δ = 5.60 (s, 1H; 1-H), 4.61 (s, 1H; 2-H), 3.90–3.41 (m, 31H), 2.78–2.69 (m, 2H), 1.69–1.55 (m, 2H), 1.46–1.36 ppm (m, 16H); UV/Vis (H₂O, 0.1 mg mL⁻¹): λ = 525 nm (surface plasmon band).

ManEG₆C₁₁-Au-GlcC₂ (30%) (3a): Reaction of a 3:5 mixture of **16** (30.0 mg, 0.048 mmol) and GlcC₂S (26.0 mg, 0.108 mmol) with HAuCl₄ (1.3 mL, 0.025 M) and NaBH₄ (620 μL, 1 N) gave **3a** (4.1 mg) as a brown powder. TEM (average diameter and number of gold atoms): 1.7 ± 0.5 nm, 201; ¹H NMR (500 MHz, D₂O): δ = 4.98 (brs, 0.3H; 1-H), 4.53 (brm, 1H; 1-H glucose), 4.13–3.25 (brm, 20H), 1.96–1.08 ppm (brm, 5.4H); UV/Vis (H₂O, 0.1 mg mL⁻¹): λ = 525 nm (surface plasmon band).

ManEG₆C₁₁-Au-GlcC₂ (15%) (3b): Reaction of a 15:85 mixture of **16** (19.0 mg, 0.030 mmol) and GlcC₂S (41.0 mg, 0.171 mmol) with HAuCl₄ (1.46 mL, 0.025 M) and NaBH₄ (800 μL, 1 N) gave **3b** (7.5 mg) as a brown powder. TEM (average diameter and number of gold atoms): 1.7 ± 0.5 nm, 201; ¹H NMR (500 MHz, D₂O): δ = 4.98 (brs; 1-H), 4.53 (brm, 1H; 1-H glucose), 4.35–3.12 (brm, 13H), 1.77–1.17 ppm (brm, 2.7H); UV/Vis (H₂O, 0.1 mg mL⁻¹): λ = 525 nm (surface plasmon band).

ManEG₆C₁₁-Au-GlcC₂ (5%) (3c): Reaction of a 5:95 mixture of **16** (6.0 mg, 0.0095 mmol) and GlcC₂S (43.0 mg, 0.179 mmol) with HAuCl₄ (1.37 mL, 0.025 M) and NaBH₄ (980 μL, 1 N) gave **3c** (8.2 mg) as a brown powder. TEM (average diameter and number of gold atoms): 1.4 ± 0.4 nm, 116; ¹H NMR (500 MHz, D₂O): δ = 5.02 (brs; 1-H), 4.54 (brm, 1H; 1-H glucose), 4.21–3.35 (brm, 10H), 1.62–1.10 ppm (brm, 0.9H); UV/Vis (H₂O, 0.1 mg mL⁻¹): λ = 525 nm (surface plasmon band).

Man₂-Au-CO₂H (66%) (4): Reaction of the disulfide mixture of **22** (29.2 mg, 0.039 mmol) in a 2:1 mannose/carboxylic acid linker ratio, HAuCl₄ (288 μL, 1 N), and NaBH₄ (158 μL, 1 N) gave **4** (7.1 mg) as a light-brown powder soluble in methanol. TEM (average diameter and number of gold atoms): 1.3 ± 0.6 nm, 38; ¹H NMR (500 MHz, D₂O): δ = 5.10 (s, 1H; 1-H), 5.04 (s, 1H; 1'-H), 4.32 (s, 1H; CH₂CO₂H), 4.09 (s, 3H), 4.01–3.32 (brm, 53H), 2.73 (brm; CH₂S), 1.95–1.26 ppm (brm, 29H); UV/Vis (H₂O, 0.1 mg mL⁻¹): surface plasmon band not observed.

Man₂-Au-CO₂H (50%) (5): Reaction of the disulfide mixture of **23'** (17.9 mg, 0.024 mol) in a 1:1 mannose/carboxylic acid linker ratio, HAuCl₄ (177 μL, 1 N), and NaBH₄ (97 μL, 1 N) gave **5** (3.2 mg) as a brown powder. TEM (average diameter and number of gold atoms): 1.0 ± 0.4 nm, 38; ¹H NMR (500 MHz, D₂O): δ = 5.14 (s, 1H; 1-H), 4.83 (s, 1H; 1'-H), 4.13–4.06 (brm, 4H), 3.99–3.32 (brm, 58H), 2.71 (brm; CH₂S), 1.98–1.19 ppm (brm, 38H); UV/Vis (H₂O, 0.1 mg mL⁻¹): surface plasmon band not observed.

Man₂-Au-CO₂H (66%) (6): Reaction of the disulfide mixture of **24** (30.4 mg, 0.036 mmol) in a 2:1 mannose/carboxylic acid linker ratio, HAuCl₄ (262 μL, 1 N), and NaBH₄ (143 μL, 1 N) gave **6** (3.5 mg) as a brown powder. TEM (average diameter and number of gold atoms): 1.3 ± 0.5 nm, 79; ¹H NMR (500 MHz, D₂O): δ = 5.29 (s, 1H; 1-H), 5.08 (s, 1H; 1'-H), 5.05 (s, 1H; 1''-H), 4.31 (s, 1H; CH₂CO₂H), 4.11 (s, 1H), 4.07 (s, 3H), 3.99–3.32 (brm, 53H), 2.76 (brs; CH₂S), 1.96–1.04 ppm (brm, 30H); UV/Vis (H₂O, 0.1 mg mL⁻¹): surface plasmon band not observed.

Man₃-Au-CO₂H (50%) (7): Reaction of the disulfide mixture of **25'** (53.5 mg, 0.077 mmol) in a 1:1 mannose/carboxylic acid linker ratio, HAuCl₄ (563 μL, 1 N), and NaBH₄ (309 μL, 1 N) gave **7** (7.1 mg) as a brown powder. TEM (average diameter and number of gold atoms): 1.3 ± 0.5 nm, 79; ¹H NMR (500 MHz, D₂O): δ = 5.13 (s, 1H; 1-H), 4.91 (s, 1H; 1'-H), 4.83 (s, 1H; 1''-H), 4.31 (s, 2H; CH₂CO₂H), 4.18–3.44 (brm, 68H), 2.79 (brs; CH₂S), 1.96–1.26 ppm (brm, 38H); UV/Vis (H₂O, 0.1 mg mL⁻¹): surface plasmon band not observed.

Man-Au (100 %) (8): Reaction of **33** (78.1 mg, 0.121 mmol) with HAuCl_4 (1.61 mL, 0.025 M) and NaBH_4 (885 μL , 1 N) gave **8** (11.1 mg) as a light-brown powder. TEM (average diameter and number of gold atoms): 1.3 ± 0.4 nm, 79; $^1\text{H NMR}$ (500 MHz, D_2O): $\delta = 4.89$ (s, 1H; 1-H), 3.98 (brs, 1H; 2-H), 3.94–3.37 (brm, 27H), 2.74 (brm; CH_2S), 1.91–0.99 ppm (brm, 18H); UV/Vis (H_2O , 0.3 mg mL^{-1}): surface plasmon band not observed; elemental analysis calcd (%) for $(\text{C}_{28}\text{H}_{55}\text{N}_2\text{O}_{10}\text{S}_2)_{40}\text{Au}_{79}$ (41 kDa): C 32.56, H 5.37, N 2.71, S 6.21; found: C 32.67, H 5.32, N 2.75, S 7.36.

Man₂-Au (100 %) (9): Reaction of **34** (30.0 mg, 0.037 mmol) with HAuCl_4 (495 μL , 0.025 M) and NaBH_4 (271 μL , 1 N) gave **9** (9.0 mg) as a light brown powder. TEM (average diameter and number of gold atoms): 1.2 ± 0.5 nm, 79; $^1\text{H NMR}$ (500 MHz, D_2O): $\delta = 5.14$ (s, 1H; 1-H), 5.05 (s, 1H; 1'-H), 4.09 (m, 1H; 2'-H), 4.05–3.45 (brm, 33H), 2.73 (brm; CH_2S), 1.74 (brm, 2H), 1.62 (brm, 2H), 1.55–1.25 ppm (brm, 14H); UV/Vis (H_2O , 0.1 mg mL^{-1}): $\lambda = 519$ nm (surface plasmon band); elemental analysis calcd (%) for $(\text{C}_{34}\text{H}_{63}\text{N}_2\text{O}_{15}\text{S}_2)_{59}\text{Au}_{79}$ (63 kDa): C 38.17, H 6.08, N 2.62, S 5.99; found: C 38.24, H 6.23, N 2.46, S 6.63.

Man₂-Au-Glc₅ (50 %) (9a): Reaction of a 1:1 mixture of **34** (22.9 mg, 0.028 mmol) and GlcC_5S (8.0 mg, 0.028 mmol) with HAuCl_4 (756 μL , 0.025 M) and NaBH_4 (415 μL , 1 N) gave **9a** (9.4 mg) as a brown powder. TEM (average diameter and number of gold atoms): 1.3 ± 0.4 nm, 79; $^1\text{H NMR}$ (500 MHz, D_2O): $\delta = 5.14$ (s, 1H; 1-H), 5.05 (s, 1H; 1'-H), 4.96–4.37 (brm, 1H; 1-H glucose), 4.09 (s, 1H; 2'-H), 4.04–3.21 (brm, 41H), 2.78 (brm; CH_2S), 1.89–0.81 ppm (brm, 24H); UV/Vis (H_2O , 0.1 mg mL^{-1}): surface plasmon band not observed; elemental analysis calcd (%) for $(\text{C}_{34}\text{H}_{63}\text{N}_2\text{O}_{15}\text{S}_2)_{22}(\text{C}_{11}\text{H}_{21}\text{O}_6\text{S})_{22}\text{Au}_{79}$ (40 kDa): C 30.12, H 4.83, N 1.56, S 5.36; found: C 29.93, H 4.88, N 1.80, S 5.93.

Man₂-Au-Glc₅ (10 %) (9b): Reaction of a 1:9 mixture of **34** (19.0 mg, 0.024 mmol) and GlcC_5S (59.7 mg, 0.211 mmol) with HAuCl_4 (3.14 mL, 0.025 M) and NaBH_4 (1.72 mL, 1 N) gave **9b** (22.5 mg) as a dark-brown powder. TEM (average diameter and number of gold atoms): 2.0 ± 0.5 nm, 225; $^1\text{H NMR}$ (500 MHz, D_2O): $\delta = 5.14$ (brs, 1H; 1-H), 5.04 (s, 1H; 1'-H), 4.47 (d, $J = 8.0$ Hz, 9H; 1-H glucose), 4.09 (brs, 2H; 2'-H), 4.03–3.22 (brm, 105H), 2.79 (t, $J = 7.5$ Hz, 2H; CH_2S), 1.88–1.28 ppm (brm, 72H); UV/Vis (H_2O , 0.1 mg mL^{-1}): $\lambda = 527$ nm (surface plasmon band); elemental analysis calcd (%) for $(\text{C}_{34}\text{H}_{63}\text{N}_2\text{O}_{15}\text{S}_2)_9(\text{C}_{11}\text{H}_{21}\text{O}_6\text{S})_{81}\text{Au}_{225}$ (74 kDa): C 19.33, H 3.10, N 0.34, S 4.27; found: C 19.31, H 3.16, N 0.69, S 4.96.

Man₃-Au-Glc₅ (50 %) (10a): Reaction of a 1:1 mixture of **35** (13.0 mg, 0.013 mmol) and GlcC_5S (3.7 mg, 0.013 mmol) with HAuCl_4 (358 μL , 0.025 M) and NaBH_4 (196 μL , 1 N) gave **10a** (4.6 mg) as a brown powder. TEM (average diameter and number of gold atoms): 1.6 ± 0.4 nm, 140; $^1\text{H NMR}$ (500 MHz, D_2O): $\delta = 5.31$ (s, 1H; 1-H), 5.12 (s, 1H; 1'-H), 5.07 (s, 1H; 1''-H), 4.52–4.21 (brm, 1H; 1-H glucose), 4.13–3.31 (brm, 48H), 2.76 (brm; CH_2S), 1.90–1.08 ppm (brm, 24H); UV/Vis (H_2O , 0.1 mg mL^{-1}): surface plasmon band not observed; elemental analysis calcd (%) for $(\text{C}_{40}\text{H}_{75}\text{N}_2\text{O}_{20}\text{S}_2)_{62}(\text{C}_{11}\text{H}_{21}\text{O}_6\text{S})_{61}\text{Au}_{140}$ (105 kDa): C 36.13, H 5.71, N 1.66, S 5.66; found: C 36.21, H 5.79, N 1.93, S 5.76.

Man₃-Au-Glc₅ (10 %) (10b): Reaction of a 1:9 mixture of **35** (6.8 mg, 0.007 mmol) and GlcC_5S (17.8 mg, 0.063 mmol) with HAuCl_4 (756 μL , 0.025 M) and NaBH_4 (513 μL , 1 N) gave **10b** (10.0 mg) as a dark-brown powder. TEM (average diameter and number of gold atoms): 1.8 ± 0.4 nm, 201; $^1\text{H NMR}$ (500 MHz, D_2O , 25 °C): $\delta = 5.32$ (s, 1H; 1-H), 5.13 (s, 1H; 1'-H), 5.06 (s, 1H; 1''-H), 4.45 (brm, 9H; 1-H glucose), 4.19–3.23 (brm, 112H), 2.18–1.08 ppm (brm, 72H); UV/Vis (H_2O , 0.1 mg mL^{-1}): surface plasmon band not observed; elemental analysis calcd (%) for $(\text{C}_{40}\text{H}_{75}\text{N}_2\text{O}_{20}\text{S}_2)_{13}(\text{C}_{11}\text{H}_{21}\text{O}_6\text{S})_{122}\text{Au}_{140}$ (86 kDa): C 25.85, H 4.12, N 0.42, S 5.49; found: C 25.89, H 4.26, N 0.54, S 5.92.

Man₄-Au-Glc₅ (50 %) (11a): Reaction of a 1:1 mixture of **36** (16.9 mg, 0.015 mmol) and GlcC_5S (4.23 mg, 0.015 mmol) with HAuCl_4 (398 μL , 0.025 M) and NaBH_4 (218 μL , 1 N) gave **11a** (6.0 mg) as a brown powder. TEM (average diameter and number of gold atoms): 1.9 ± 0.5 nm, 225; $^1\text{H NMR}$ (500 MHz, D_2O): $\delta = 5.38$ (brs, 1H), 5.33 (brs, 1H), 5.08 (s, 1H), 4.86 (s, 1H), 4.47 (d, $J = 7.5$ Hz, 1H; 1-H glucose), 4.24–3.31 (brm, 54H), 1.81–1.13 ppm (brm, 24H); UV/Vis (H_2O , 0.1 mg mL^{-1}): $\lambda = 520$ nm (surface plasmon band); elemental analysis calcd (%) for $(\text{C}_{46}\text{H}_{85}\text{N}_2\text{O}_{25}\text{S}_2)_{56}(\text{C}_{11}\text{H}_{21}\text{O}_6\text{S})_{56}\text{Au}_{225}$ (123 kDa): C 31.08, H 4.85, N 1.27, S 4.37; found: C 31.23, H 5.09, N 1.94, S 4.63.

Man₄-Au-Glc₅ (10 %) (11b): Reaction of a 1:9 mixture of **36** (11.4 mg, 0.010 mmol) and GlcC_5S (25.4 mg, 0.09 mmol) with HAuCl_4 (1.344 mL, 0.025 M) and NaBH_4 (738 μL , 1 N) gave **11b** (13.0 mg) as a brown powder. TEM (average diameter and number of gold atoms): 1.4 ± 0.7 nm, 116; $^1\text{H NMR}$ (500 MHz, D_2O): $\delta = 5.28$ (brs, 1H), 5.23 (brs, 1H), 4.97 (brs, 1H), 4.71 (brs, 1H, partially overlapped by water signal), 4.36 (brm, 9H; 1-H glucose), 4.10–3.13 (brm, 118H), 1.87–1.10 ppm (brm, 72H); UV/Vis (H_2O , 0.1 mg mL^{-1}): $\lambda = 527$ nm (surface plasmon band); elemental analysis calcd (%) for $(\text{C}_{46}\text{H}_{85}\text{N}_2\text{O}_{25}\text{S}_2)_{7}(\text{C}_{11}\text{H}_{21}\text{O}_6\text{S})_{59}\text{Au}_{116}$ (47 kDa): C 24.63, H 3.90, N 0.41, S 4.94; found: C 24.40, H 4.36, N 0.77, S 4.53.

Man₅-Au-Glc₅ (50 %) (12a): Reaction of a 1:1 mixture of **37** (14.0 mg, 0.011 mmol) and GlcC_5S (3.05 mg, 0.011 mmol) with HAuCl_4 (288 μL , 0.025 M) and NaBH_4 (158 μL , 1 N) gave **12a** (4.4 mg) as a brown powder. TEM (average diameter and number of gold atoms): 2.1 ± 1.5 nm, 309; $^1\text{H NMR}$ (500 MHz, D_2O): $\delta = 5.37$ (s, 1H), 5.16 (s, 1H), 5.08 (s, 1H), 5.06 (s, 1H), 4.86 (s, 1H), 4.43 (brm, 1H; 1-H glucose), 4.23–3.18 (brm, 60H), 2.75 (brm; CH_2S), 1.89–1.13 ppm (brm, 24H); UV/Vis (H_2O , 0.1 mg mL^{-1}): surface plasmon band not observed; elemental analysis calcd (%) for $(\text{C}_{52}\text{H}_{95}\text{N}_2\text{O}_{30}\text{S}_2)_{28}(\text{C}_{11}\text{H}_{21}\text{O}_6\text{S})_{28}\text{Au}_{309}$ (105 kDa): C 20.19, H 3.12, N 0.71, S 2.57; found: C 20.12, H 3.53, N 0.89, S 3.03.

Man₅-Au-Glc₅ (10 %) (12b): Reaction of a 1:9 mixture of **37** (5.75 mg, 0.0044 mmol) and GlcC_5S (11.3 mg, 0.040 mmol) with HAuCl_4 (593 μL , 0.025 M) and NaBH_4 (326 μL , 1 N) gave **12b** (5.3 mg) as a dark-brown powder. TEM (average diameter and number of gold atoms): 1.8 ± 0.3 nm, 201 (double distribution: a small percentage of the GNPs have an average diameter of 5 nm); $^1\text{H NMR}$ (500 MHz, D_2O): $\delta = 5.37$ (s, 1H), 5.17 (s, 1H), 5.08 (s, 1H), 5.06 (s, 1H), 4.85 (s, 1H), 4.42–4.33 (brm, 9H; 1-H glucose), 4.19–3.90 (brm, 124H), 2.12–1.26 ppm (brm, 72H); UV/Vis (H_2O , 0.1 mg mL^{-1}): surface plasmon band not observed; elemental analysis calcd (%) for $(\text{C}_{52}\text{H}_{95}\text{N}_2\text{O}_{30}\text{S}_2)_{5}(\text{C}_{11}\text{H}_{21}\text{O}_6\text{S})_{43}\text{Au}_{201}$ (58 kDa): C 15.14, H 2.39, N 0.24, S 2.92; found: C 14.96, H 2.80, N 0.35, S 2.93.

Man₇-Au-Glc₅ (50 %) (13a): Reaction of a 1:1 mixture of **38** (10.49 mg, 0.0065 mmol) and GlcC_5S (1.83 mg, 0.0065 mmol) with HAuCl_4 (173 μL , 0.025 M) and NaBH_4 (95 μL , 1 N) gave **13a** (6.2 mg) as a brown powder. TEM (average diameter and number of gold atoms): 1.8 ± 0.4 nm, 201; $^1\text{H NMR}$ (500 MHz, D_2O): $\delta = 5.37$ (s, 1H), 5.32 (brs, 2H), 5.14 (s, 1H), 5.07 (s, 2H) (one anomeric signal overlapped by the solvent signal), 4.21–3.16 (brm, 72H), 2.77 (brm; CH_2S), 1.88–1.13 ppm (brm, 24H); UV/Vis (H_2O , 0.1 mg mL^{-1}): surface plasmon band not observed; elemental analysis calcd (%) for $(\text{C}_{52}\text{H}_{95}\text{N}_2\text{O}_{30}\text{S}_2)_{58}(\text{C}_{11}\text{H}_{21}\text{O}_6\text{S})_{58}\text{Au}_{201}$ (150 kDa): C 34.91, H 5.31, N 1.09, S 3.73; found: C 34.93, H 5.75, N 1.66, S 3.51.

Acknowledgements

The work was supported by the EU (grants EMPRO LSHP-CT2003-503558 and Glycogold MRTN-CT2004-005645), the Spanish Ministry of Education and Science (MEC, grant CTQ2008-04638), and the Fondation Dormeur. O.M.A. thanks the CSIC (I3P program) and MEC for financial support.

- [1] M. Mammen, S.-K. Choi, G. M. Whitesides, *Angew. Chem.* **1998**, *110*, 2908–2953; *Angew. Chem. Int. Ed.* **1998**, *37*, 2754–2794.
- [2] Y. C. Lee, R. T. Lee, *Acc. Chem. Res.* **1995**, *28*, 321–327.
- [3] L. L. Kiessling, J. K. Pontrello, M. C. Schuster, in *Carbohydrate-Based Drug Discovery* (Ed.: C.-H. Wong), Wiley-VCH, Weinheim, **2003**, pp. 575–609.
- [4] J. M. de La Fuente, A. G. Barrientos, T. C. Rojas, J. Rojo, J. Cañada, A. Fernández, S. Penadés, *Angew. Chem.* **2001**, *113*, 2317–2321; *Angew. Chem. Int. Ed.* **2001**, *40*, 2257–2261.
- [5] A. G. Barrientos, J. M. de La Fuente, T. C. Rojas, A. Fernández, S. Penadés, *Chem. Eur. J.* **2003**, *9*, 1909–1921.
- [6] J. M. de La Fuente, S. Penadés, *BBA-Gen. Subjects* **2006**, *1760*, 636–651.
- [7] J. M. de La Fuente, S. Penadés, *Glycoconjugate J.* **2004**, *21*, 149–163.

- [8] J. Rojo, V. Díaz, J. M. de La Fuente, I. Segura, A. G. Barrientos, H. H. Riese, A. Bernad, S. Penadés, *ChemBioChem* **2004**, *5*, 291–297.
- [9] a) T. Mizuochi, M. W. Spellman, M. Larkin, J. Solomon, L. J. Basa, T. Feizi, *Biochem. J.* **1988**, *254*, 599–603; b) T. Feizi, M. Larkin, *Glycobiology* **1990**, *1*, 17–23; c) E. Fenouillet, J. C. Gluckman, I. M. Jones, *Trends Biochem. Sci.* **1994**, *19*, 65–70; d) H. Geyer, C. Holschbach, G. Hunsmann, J. Schneider, *J. Biol. Chem.* **1988**, *263*, 11760–11767; e) J. Lifson, S. Coutre, E. Huang, E. Engleman, *J. Exp. Med.* **1986**, *164*, 2101–2106; f) T. Mizuochi, M. W. Spellman, M. Larkin, J. Solomon, L. J. Basa, T. Feizi, *Biomed. Chromatogr.* **1987**, *2*, 260–270; g) T. Mizuochi, T. J. Matthews, M. Kato, J. Hamako, K. Titani, J. Solomon, T. Feizi, *J. Biol. Chem.* **1990**, *265*, 8519–8524.
- [10] a) R. Wyatt, J. Sodroski, *Science* **1998**, *280*, 1884–1888; b) R. Wyatt, P. D. Kwong, E. Desjardins, R. W. Sweet, J. Robinson, W. A. Hendrickson, J. G. Sodroski, *Nature* **1998**, *393*, 705–711.
- [11] M. Zhang, B. Gaschen, W. Blay, B. Foley, N. Haigwood, C. Kuiken, B. Korber, *Glycobiology* **2004**, *14*, 1229–1246.
- [12] T. B. H. Geijtenbeek, R. Torensma, S. J. van Vliet, G. C. F. van Duijnhoven, G. J. Adema, Y. van Kooyk, C. G. Figdor, *Cell* **2000**, *100*, 575–584.
- [13] S. Pöhlman, F. Baribaud, R. D. Doms, *Trends Immunol.* **2001**, *22*, 643–646.
- [14] Y. van Kooyk, T. B. H. Geijtenbeek, *Nat. Rev. Immunol.* **2003**, *3*, 697–709.
- [15] B. M. Curtis, S. Scharnowske, A. J. Watson, *Proc. Natl. Acad. Sci. USA* **1992**, *89*, 8356–8360.
- [16] H. Feinberg, D. A. Mitchell, K. Drickamer, W. I. Weis, *Science* **2001**, *294*, 2163–2166.
- [17] Y. Guo, H. Feinberg, E. Conroy, D. A. Mitchell, R. Alvarez, O. Blixt, M. E. Taylor, W. I. Weis, K. Drickamer, *Nat. Struct. Mol. Biol.* **2004**, *11*, 591–598.
- [18] K. D. McReynolds, J. Gervay-Hague, *Chem. Rev.* **2007**, *107*, 1533–1552.
- [19] C. N. Scanlan, J. Offer, N. Zitzmann, R. A. Dwek, *Nature* **2007**, *446*, 1038–1045.
- [20] a) J.-E. Hansen, H. Clausen, C. Nielsen, L. S. Teglbjærg, L. L. Hansen, C. M. Nielsen, E. Dabelsteen, L. Mathiesen, S.-I. Hakomori, J. O. Nielsen, *J. Virol.* **1990**, *64*, 2833–2840; b) J.-E. Hansen, C. Nielsen, M. Arendrup, S. Olofsson, L. Mathiesen, J. O. Nielsen, H. Clausen, *J. Virol.* **1991**, *65*, 6461–6467; c) J.-E. S. Hansen, C. M. Nielsen, C. Nielsen, P. Heegaard, L. R. Mathiesen, J. O. Nielsen, *AIDS* **1989**, *3*, 635–642; d) A. Pashov, M. Perry, M. Dyar, M. Chow, T. Kieber-Emmons, *Curr. Pharm. Des.* **2007**, *13*, 185–201.
- [21] D. A. Calarese, H.-K. Lee, C.-Y. Huang, M. D. Best, R. D. Astronomo, R. L. Stanfield, H. Katinger, D. R. Burton, C.-H. Wong, I. A. Wilson, *Proc. Natl. Acad. Sci. USA* **2005**, *102*, 13371–13377.
- [22] E. W. Adams, D. M. Ratner, P. H. Seeberger, N. Hacohen, *ChemBioChem* **2008**, *9*, 294–303.
- [23] J. Wang, H. Li, G. Zou L.-X. Wang, *Org. Biomol. Chem.* **2007**, *5*, 1529–1540.
- [24] N. Frison, M. E. Taylor, E. Soilleux, M.-T. Bousser, R. Mayer, M. Monsigny, K. Drickamer, A.-C. Roche, *J. Biol. Chem.* **2003**, *278*, 23922–23929.
- [25] S.-K. Wang, P.-L. Liang, R. D. Astronomo, T.-L. Hsu, S.-L. Hsieh, D. R. Burton, C.-H. Wong, *Proc. Natl. Acad. Sci. USA* **2008**, *105*, 3690–3695.
- [26] G. Tabarani, J. J. Reina, C. Ebel, C. Vives, H. Lortat-Jacob, J. Rojo, F. Fieschi, *FEBS Lett.* **2006**, *580*, 2402–2408.
- [27] R. Ojeda, J. L. de Paz, A. G. Barrientos, M. Martín-Lomas, S. Penadés, *Carbohydr. Res.* **2007**, *342*, 448–459.
- [28] J. G. Joyce, I. J. Krauss, H. C. Song, D. W. Opalka, K. M. Grimm, D. D. Nahas, M. T. Esser, R. Hrin, M. Feng, V. Y. Dudkin, M. Chastain, J. W. Shiver, S. J. Danishefsky, *Proc. Natl. Acad. Sci. USA* **2008**, *105*, 15684–15689.
- [29] a) V. Y. Dudkin, M. Orlova, X. Geng, M. Mandal, W. C. Olson, S. J. Danishefsky, *J. Am. Chem. Soc.* **2004**, *126*, 9560–9562; b) L.-X. Wang, J. Ni, S. Singh, H. Li, *Chem. Biol.* **2004**, *11*, 127–134; c) J. Ni, H. Song, Y. Wang, N. M. Stamatou, L.-X. Wang, *Bioconjugate Chem.* **2006**, *17*, 493–500.
- [30] H. Li, L.-X. Wang, *Org. Biomol. Chem.* **2004**, *2*, 483–488.
- [31] a) L. Bédouet, M.-T. Bousser, N. Frison, C. Boccaccio, J.-P. Abastado, P. Marceau, R. Mayer, M. L. Monsigny, A.-C. Roche, *Biosci. Rep.* **2001**, *21*, 839–855; b) N. Frison, P. Marceau, A.-C. Roche, M. Monsigny, R. Mayer, *Biochem. J.* **2002**, *368*, 111–119.
- [32] a) T. Ogawa, K. Kiyooki, K. Sasajima, M. Matsui, *Tetrahedron* **1981**, *37*, 2779–2786; b) T. Ogawa, K. Sasajima, *Tetrahedron* **1981**, *37*, 2787–2792; c) T. Ogawa, K. Sasajima, *Carbohydr. Res.* **1981**, *93*, 53–66; d) T. Ogawa, S. Nakabayashi, T. Kitajima, *Carbohydr. Res.* **1983**, *114*, 225–236; e) T. Ogawa, T. Nukada, *Carbohydr. Res.* **1985**, *136*, 135–152; f) J. R. Merritt, E. Naisang, B. Fraser-Reid, *J. Org. Chem.* **1994**, *59*, 4443–4449; g) P. Grice, S. V. Ley, J. Pietruszka, H. Priepeke, *Angew. Chem.* **1996**, *108*, 206–208; *Angew. Chem. Int. Ed. Engl.* **1996**, *35*, 197–200; h) P. Grice, S. V. Ley, J. Pietruszka, H. Osborn, H. Priepeke, S. Warriner, *Chem. Eur. J.* **1997**, *3*, 431–440; i) H.-K. Lee, C. N. Scanlan, C.-Y. Huang, A. Y. Chang, D. A. Calarese, R. A. Dwek, P. M. Rudd, D. R. Burton, I. A. Wilson, C.-H. Wong, *Angew. Chem.* **2004**, *116*, 1018–1021; *Angew. Chem. Int. Ed.* **2004**, *43*, 1000–1003.
- [33] For an exhaustive review about thiolate SAMs on metals, see: J. C. Love, L. A. Estroff, J. K. Kriebel, R. G. Nuzzo, G. M. Whitesides, *Chem. Rev.* **2005**, *105*, 1103–1169.
- [34] M. Mrksich, G. M. Whitesides, *Annu. Rev. Biophys. Biomol. Struct.* **1996**, *25*, 55–78.
- [35] For information on the importance of PEG chain synthesis, see: F. A. Loiseau, K. K. (Mimi) Hii, A. M. Hill, *J. Org. Chem.* **2004**, *69*, 639–647, and references therein.
- [36] D. J. Revell, J. R. Knight, D. J. Blyth, A. H. Haines, D. A. Russell, *Langmuir* **1998**, *14*, 4517–4524.
- [37] C.-C. Lin, Y.-C. Yeh, C.-Y. Yang, C.-L. Chen, G.-F. Chen, C.-C. Chen, Y.-C. Wu, *J. Am. Chem. Soc.* **2002**, *124*, 3508–3509.
- [38] B. Fraser-Reid, U. E. Udodong, Z. Wu, H. Ottosson, J. R. Merritt, C. S. Rao, C. Roberts, R. Madsen, *Synlett* **1992**, 927–942.
- [39] K. P. R. Kartha, H. J. Jennings, *J. Carbohydr. Chem.* **1990**, *9*, 777–781.
- [40] C. Pale-Grosdemange, E. S. Simon, K. L. Prime, G. M. Whitesides, *J. Am. Chem. Soc.* **1991**, *113*, 12–20.
- [41] A. García-Barrientos, J. J. García-Lopéz, J. Isac-García, F. Ortega-Caballero, C. Uriel, A. Bargas Berenguer, F. Santoyo-González, *Synthesis* **2001**, 1057–1064.
- [42] G. Zemplén, *Ber. Dtsch. Chem. Ges.* **1927**, *60*, 1555–1564.
- [43] T. Buskas, E. Söderberg, P. Konradsson, B. Fraser-Reid, *J. Org. Chem.* **2000**, *65*, 958–963.
- [44] We followed the experimental procedure used for similar substrates by B. Frisch et al., see: B. Frisch, C. Boeckler, F. Schuber, *Bioconjugate Chem.* **1996**, *7*, 180–186.
- [45] E. Arce, P. M. Nieto, V. Díaz, R. García Castro, A. Bernard, J. Rojo, *Bioconjugate Chem.* **2003**, *14*, 817–823.
- [46] For other published routes to compound **27**, see: a) T. K. Lindhorst, S. Kötter, U. Krallmann-Wenzel, S. Ehlers, *J. Chem. Soc. Perkin Trans. 1* **2001**, 823–831; b) L. E. Strong, L. L. Kiessling, *J. Am. Chem. Soc.* **1999**, *121*, 6193–6196; c) N. Jayaraman, J. F. Stoddart, *Tetrahedron Lett.* **1997**, *38*, 6767–6770.
- [47] In the Wong protocol (ref. [32i]), the oligosaccharides were obtained as aminopentyl (instead of aminoethyl) derivatives.
- [48] G. V. S. Reddy, G. V. Rao, R. V. K. Subramanyam, D. S. Iyengar, *Synth. Commun.* **2000**, *30*, 2233–2237.
- [49] A. Koziara, *J. Chem. Res.* **1989**, 296–297.
- [50] M. J. Hostetler, J. E. Wingate, C.-J. Zhong, J. E. Harris, R. W. Vachet, M. R. Clark, J. D. Londono, S. J. Green, J. J. Stokes, G. D. Wignall, G. L. Glish, M. D. Porter, N. D. Evans, R. W. Murray, *Langmuir* **1998**, *14*, 17–30.
- [51] H. Feinberg, R. Castelli, K. Drickamer, P. H. Seeberger, W. I. Weis, *J. Biol. Chem.* **2006**, *282*, 4202–4209.
- [52] A. Alfsen, M. Bomsel, *J. Biol. Chem.* **2002**, *277*, 25649–25659.
- [53] X. Wang, P. Sun, A. Al-Qamari, T. Tai, I. Kawashima, A. S. Paller, *J. Biol. Chem.* **2001**, *276*, 8436–8444.

- [54] a) M. Moulard, H. Lortat-Jacob, I. Mondor, G. Roca, R. Wyatt, J. Sodroski, L. Zhao, W. Olson, P. D. Kwong, Q. J. Sattentau, *J. Virol.* **2000**, *74*, 1948–1960; b) L. N. Callahan, M. Phelan, M. Mallinson, M. A. Norcross, *J. Virol.* **1991**, *65*, 1543–1550; c) A. R. Neurath, N. Strick, Y. Y. Li, *BMC Infect. Dis.* **2002**, *2*, 27.
- [55] A. Cambi, C. G. Figdor, *Curr. Opin. Immunol.* **2005**, *17*, 345–351.
- [56] For highlights on the design of HIV vaccines, see: a) L.-X. Wang, in *Carbohydrate Drug Design* (Eds.: A. A. Klyosov, Z. J. Witczak, D. Platt), Oxford University Press, Oxford, **2006**, pp. 133–160; b) D. Calarese, C. Escalan, H.-K. Lee, P. Rudd, C.-H. Wong, R. Dwek, D. Burton, I. A. Wilson, in *Carbohydrate Drug Design* (Eds.: A. A. Klyosov, Z. J. Witczak, D. Platt), Oxford University Press, Oxford, **2006**, pp. 161–185, and references therein.
- [57] D. A. Mitchell, A. J. Fadden, K. Drickamer, *J. Biol. Chem.* **2001**, *276*, 28939–28945.
- [58] P. Y. Lozach, H. Lortat-Jacob, L. A. de Lacroix, I. Staropoli, S. Foung, A. Amara, C. Houles, F. Fieschi, O. Schwartz, J. L. Virelizier, F. Arenzana-Seisdedos, R. Altmeyer, *J. Biol. Chem.* **2003**, *278*, 20358–20366.
- [59] BIAtechnology Handbook, BIACORE AB, Uppsala, **1998**.

Received: April 7, 2009
Published online: August 13, 2009